

**OFFICE OF CIVILIAN RADIOACTIVE WASTE MANAGEMENT  
ANALYSIS/MODEL COVER SHEET**

1. QA: QA

Page: 1 of 53

*Complete Only Applicable Items*

2.  Analysis      Check all that apply

Type of Analysis	<input type="checkbox"/> Engineering <input type="checkbox"/> Performance Assessment <input checked="" type="checkbox"/> Scientific
Intended Use of Analysis	<input type="checkbox"/> Input to Calculation <input checked="" type="checkbox"/> Input to another Analysis or Model <input type="checkbox"/> Input to Technical Document <input type="checkbox"/> Input to Other Technical Products
Describe use: Provides parameters on volcanic eruption dynamics and intrusion geometry for use in igneous consequence analyses.	

3.  Model      Check all that apply

Type of Model	<input type="checkbox"/> Conceptual Model <input type="checkbox"/> Abstraction Model <input type="checkbox"/> Mathematical Model <input type="checkbox"/> System Model <input type="checkbox"/> Process Model
Intended Use of Model	<input type="checkbox"/> Input to Calculation <input type="checkbox"/> Input to another Model or Analysis <input type="checkbox"/> Input to Technical Document <input type="checkbox"/> Input to Other Technical Products
Describe use:	

4. Title:  
Characterize Eruptive Processes at Yucca Mountain, Nevada

5. Document Identifier (including Rev. No. and Change No., if applicable):  
ANL-MGR-GS-000002, Rev 00

6. Total Attachments: none      7. Attachment Numbers - No. of Pages in Each:

	Printed Name	Signature	Date
8. Originator	Greg Valentine Stephen Nelson		25 Apr 00
9. Checker	Schön Levy		04/25/2000
10. Lead/Supervisor	Debra Bryan		4/26/2000
11. Responsible Manager	Debra Bryan		4/26/2000

12. Remarks:

**INFORMATION ONLY**

**PRELIMINARY DRAFT  
INFORMATION ONLY**

*ADD: Manny Comar WM-11 JFD3*

**OFFICE OF CIVILIAN RADIOACTIVE WASTE MANAGEMENT  
ANALYSIS/MODEL REVISION RECORD**

*Complete Only Applicable Items*

1. Page: 2 of: 53

2. Analysis or Model Title:

Characterize Eruptive Processes at Yucca Mountain, Nevada

3. Document Identifier (including Rev. No. and Change No., if applicable):

ANL-MGR-GS-000002, Rev 00

4. Revision/Change No.

5. Description of Revision/Change

00

Initial Issue

## **DRAFT DISCLAIMER**

This contractor document was prepared for the U.S. Department of Energy (DOE), but has not undergone programmatic, policy, or publication review, and is provided for information only. The document provides preliminary information that may change based on new information or analysis, and is not intended for publication or wide distribution; it is a lower level contractor document that may or may not directly contribute to a published DOE report. Although this document has undergone technical reviews at the contractor organization, it has not undergone a DOE policy review. Therefore, the views and opinions of authors expressed do not necessarily state or reflect those of the DOE. However, in the interest of the rapid transfer of information, we are providing this document for your information, per your request.

# CONTENTS

	Page
1. PURPOSE .....	11
2. QUALITY ASSURANCE .....	13
3. COMPUTER SOFTWARE AND MODEL USAGE .....	15
4. INPUTS .....	17
4.1 DATA AND PARAMETERS .....	17
4.2 CRITERIA .....	19
4.3 CODES AND STANDARDS .....	19
5. ASSUMPTIONS .....	21
6. ANALYSIS/MODEL .....	25
6.1 CHARACTERISTICS OF ERUPTIVE CONDUITS, DIKE WIDTHS, AND DIKE SWARMS .....	25
6.2 CHARACTERISTICS OF IGNEOUS MATERIAL .....	26
6.2.1 Magma Chemistry .....	26
6.2.2 Water Content .....	28
6.2.3 Mole Percent of Constituents in Volcanic Gas .....	29
6.2.4 Magmatic Temperatures, Viscosities, and Densities .....	30
6.3 ERUPTIVE PROCESSES .....	32
6.3.1 Magma Ascent Rate Below Volatile Exsolution .....	34
6.3.2 Volatile Exsolution and Fragmentation .....	34
6.3.3 Velocity as a Function of Depth Above $d_{exs}$ .....	39
6.3.4 Eruption Duration and Volume .....	39
6.4 ENTRAINMENT OF RADIOACTIVE WASTE IN ASCENDING MAGMA .....	42
6.5 ASH PLUMES AND THEIR DEPOSITS .....	43
6.5.1 Bulk Particle Size and Distribution of Deposits from Strombolian and Violent Strombolian Eruptions .....	43
6.5.2 Clast Characteristics .....	44
6.5.3 Density of Fallout Deposits .....	45
7. CONCLUSIONS .....	47

8. INPUTS AND REFERENCES .....	49
8.1 DOCUMENTS CITED .....	49
8.2 CODES, STANDARDS, REGULATIONS, AND PROCEDURES.....	53
8.3 SOURCE DATA, LISTED BY DATA TRACKING NUMBERS .....	53

## FIGURES

	Page
1. Plot of the Depth at Which Volatile ( $H_2O$ ) Exsolution Begins for Initial Dissolved Water Content up to 0.05 ..... <div style="display: flex; justify-content: space-between; margin-left: 20px; margin-top: -10px;"> <span><math>(n_i)</math> DSB 5/1/00</span> <span><math>(d_{exs})</math> DSB 5/1/00</span> </div>	36
2. Plot of the Variation of Gas Volume Fraction with Depth, Assuming Pressure in the Magma is Lithostatic, for Initial Dissolved Water Content $n_i = 0.01, 0.02, 0.03, 0.04,$ and 0.05. .... <div style="display: flex; justify-content: space-around; margin-left: 20px; margin-top: -10px;"> <span><math>(\phi)</math> DSB 5/1/00</span> <span><math>(d)</math> DSB 5/1/00</span> </div>	38
3. Plot of the Variation of Eruption Velocity with Initial Dissolved Water Content for Various Mass Discharge Rates Along a Fissure ..... <div style="display: flex; justify-content: space-between; margin-left: 20px; margin-top: -10px;"> <span><math>(u_{erupt})</math> DSB 5/1/00</span> <span><math>(n_i)</math> DSB 5/1/00</span> </div>	40
4. Plot of the Variation of Eruption Velocity with Initial Dissolved Water Content for Various Mass Discharge Rates from a Circular Conduit. .... <div style="display: flex; justify-content: space-between; margin-left: 20px; margin-top: -10px;"> <span><math>(u_{erupt})</math> DSB 5/1/00</span> <span><math>(n_i)</math> DSB 5/1/00</span> </div>	41

INTENTIONALLY LEFT BLANK

## TABLES

	Page
1a. Summary of Data <sup>OSB 5/1/00</sup> and Parameters Used as Inputs for Calculations in this AMR.....	17
1b. Summary of Sources of Information Used as Technical Product Inputs to Support Methodologies, Assumptions, and Calculations in this AMR .....	17-18
<sup>OSB 5/1/00</sup> 2. Mean Lathrop Wells Lava Chemistry with Associated Statistics .....	27-28
3. Mole Percent Concentration of Volcanic Gases and Associated Uncertainty Estimates .....	30
4. Calculated Saturation Pressures and Temperatures as a Function of Water Content for Lathrop Wells Magmas.....	32
5. Explosive Eruptive Events, Duration, and Power and Estimated Mass Discharge Rates Used to Develop Probability Distributions for Eruptive Plume Dispersal Calculations .....	41
6. Estimated Bulk Clast Size Distribution Parameters for Three Violent Strombolian Eruptions (Tolbachik and Cerro Negro 1971 and 1968) and One Strombolian Eruption (Etna 1971).....	44

INTENTIONALLY LEFT BLANK

## ACRONYMS

AMOPE	Assistant Manager, Office of Project Execution
AMR	Analysis/Model Report
CRWMS M&O	Civilian Radioactive Waste Management System Management and Operating Contractor
DOE	Department of Energy
DTN	Data tracking number
OCRWM	Office of Civilian Radioactive Waste Management
PMR	Process Model Report
QA	Quality assurance
QARD	Quality Assurance Requirements and Description
N/A	Not applicable
PA	Performance assessment
PMR	Process Model Report
SR	Site Recommendation
TBV	To be verified
TSPA	Total System Performance Assessment
YMP	Yucca Mountain Site Characterization Project
YMR	Yucca Mountain region

INTENTIONALLY LEFT BLANK

## 1. PURPOSE

This Analysis/Model Report (AMR), *Characterize Eruptive Processes at Yucca Mountain, Nevada*, presents information about natural volcanic systems and the parameters that can be used to model their behavior. This information is used to develop parameter-value distributions appropriate for analysis of the consequences of volcanic eruptions through a potential repository at Yucca Mountain. Within the framework of the Disruptive Events Process Model Report (PMR), this AMR provides information for the calculations in two other AMRs (CRWMS M&O 2000a and b); parameters described herein are directly used in calculations in these reports (e.g., using the ASHPLUME atmospheric dispersal code in CRWMS M&O (2000b,)) and will be used in Total System Performance Assessment (TSPA). Compilation of this AMR was conducted as defined in the Development Plan (CRWMS M&O 1999a), except as noted below.

The report begins with considerations of the geometry of volcanic feeder systems, which are of primary importance in predicting how much of a potential repository would be affected by an eruption. This discussion is followed by one of the physical and chemical properties of the magmas, which influences both eruptive styles and mechanisms for interaction with radioactive waste packages. Eruptive processes including the ascent velocity of magma at depth, the onset of bubble nucleation and growth in the rising magmas, magma fragmentation, and velocity of the resulting gas-particle mixture are then discussed. The duration of eruptions, their power output, and mass discharge rates are also described. The next section summarizes geologic constraints regarding the interaction between magma and waste packages. Finally, we discuss the bulk grain size produced by relevant explosive eruptions and grain shapes.

Section 3.1 of the Development Plan (CRWMS M&O 1999a) contains the following statements:

“The report will describe the entrainment of radioactive waste particles by ascending magma.”

“...the report will describe the chemical and mineralogical forms of ash and waste that are deposited.”

Section 3.3 of the same Development Plan contains the following statements:

“Synthesize information from Project and external sources to describe the entrainment of radioactive waste within ascending magma or pyroclastic material at Yucca Mountain, including particle size, shape, and density.”

“Properties to be addressed include ... waste particle characteristics. In addition, information on environmental conditions will also be required.”

Information pertaining specifically to waste (composition, particle size, and entrainment by rising magma) and to environmental conditions (e.g., wind velocities) are not described in this AMR but in CRWMS M&O (2000b).

Section 12.0 of the same Development Plan (CRWMS M&O 1999a) states that the only computer software used in this AMR will be the ASHPLUME code. However, ASHPLUME is not used here but is described in CRWMS M&O (2000b).

## 2. QUALITY ASSURANCE

The activities documented in this AMR were evaluated in accordance with QAP-2-0, *Conduct of Activities*, and were determined to be subject to the requirements of the U.S. Department of Energy (DOE) Office of Civilian Radioactive Waste Management (OCRWM) *Quality Assurance Requirements and Description* (QARD) (DOE 2000). This evaluation is documented in CRWMS M&O 1999b and in *Activity Evaluation for Work Package WP 1401213DMI* (attachment in Wemheuer 1999). This AMR has been prepared in accordance with procedure AP-3.10Q, *Analyses and Models*. The conclusions in this AMR do not affect the repository design or permanent items as discussed in QAP-2-3, *Classification of Permanent Items*.

INTENTIONALLY LEFT BLANK

### **3. COMPUTER SOFTWARE AND MODEL USAGE**

Standard, built-in functions of Microsoft Excel, V5.0a, for Macintosh were used to calculate parameters in Tables 2, 3, and 4. All other calculations were done using a hand-held calculator. No numerical models were used to produce this report.

INTENTIONALLY LEFT BLANK

## 4. INPUTS

In this AMR, pertinent scientific literature is reviewed and some simple theoretical concepts are developed. This information is used to suggest parameter distributions for use in Yucca Mountain Site Characterization Project (YMP) TSPA calculations. Where possible, parameter distributions are based on data or models available in published sources. In cases for which there are insufficient published data, parameter distributions are suggested that conservatively capture the expected range based on the judgement of the authors.

### 4.1 DATA AND PARAMETERS

Locations and brief descriptions of data and assumed values that were used as input for this AMR are listed in Table 1a. Locations and descriptions of information inputs to support methodologies, assumptions, and calculations in this AMR are listed in Table 1b and discussed in Section 5. Qualification status of the inputs is indicated in the Document Input Reference System database.

Table 1a. Summary of Data Used as Inputs for Calculations in this AMR

Data Used	Application of Data	Data Sources	Location in this AMR
45 chemical analyses of products from Lathrop Wells volcano.	Calculation of mean chemical composition of Lathrop Wells products.	DTN: LA00000000099.002	Section 6.2.1
Xenolith contents at Alkali Buttes and Volcano Hill.	Discussion of geologic constraints on entrainment of waste.	DTN: LAGV831812AQ97.001	Section 6.4

Table 1b. Summary of Sources of Information Used as Technical Product Inputs to Support Methodologies, Assumptions, and Calculations in this AMR

Information Used	Application of Information	Sources	Location in this AMR
Discussion of Lathrop Wells volcano conduit diameter. Xenolith (lithic) content at Lathrop Wells volcano.	Development of distribution of conduit diameters for potential volcano in Yucca Mountain Region. Discussion of entrainment of waste during a potential eruption.	Doubik and Hill (1999, pp. 60-61)	Sections 6.1, 6.4
Diameter of Grants Ridge plug.	Development of distribution of conduit diameters for potential volcano in Yucca Mountain Region.	Keating and Valentine (1998, p. 41); Woldegabriel et al. (1999, p. 392)	Section 6.1
Dike width measurements in Yucca Mountain Region. Ratios of fallout sheet volume to cone volume for violent strombolian eruptions.	Comparison with dike width distribution suggested in this AMR. Discussion of characteristics of fallout and cone deposits from violent strombolian eruptions.	Crowe et al. (1983, pp. 266, 272)	Section 6.1, 6.5.1
Experimental constraints on water content of basaltic magmas.	Constraints in developing distribution for water content of potential volcano in Yucca Mountain Region.	Knutson and Green (1975, Fig. 1, p. 126)	Section 6.2.2, 6.2.4

Table 1b (continued)

Relationship between temperature and composition for basaltic magmas.	Calculation of temperatures of magmas forming potential Yucca Mountain Region volcanoes.	Sisson and Grove (1993a, pp. 163, 167)	Sections 6.2.2, 6.2.4
Composition of gases from eight historically active volcanoes.	Calculation of mean gas composition and associated uncertainty.	Symonds et al. (1994, Tables 3–5)	Section 6.2.3
Equation relating water saturation to pressure in basaltic magmas.	Calculation of saturation pressures, exsolution depths, and volume fraction of gas in magma as a function of pressure.	Jaupart and Tait (1990, p. 219)	Sections 6.2.4, 6.3.2
Method for calculating magma viscosity as a function of composition.	Calculation of viscosities of magmas forming potential Yucca Mountain Region volcanoes.	Shaw (1972, pp. 873, 878)	Section 6.2.4
Equation for density of basic magmas.	Calculation of magma density for potential Yucca Mountain Region volcanoes.	Ochs and Lange (1999, p. 1314, Eq. 2)	Section 6.2.4
Estimate of magma flow rate necessary to form aa lavas.	Discussion of constraints on magma discharge rates at Yucca Mountain Region volcanoes.	Rowland and Walker (1990, p. 626)	Section 6.3
Theoretical equations and results describing the ascent of basaltic magmas.	Equation for velocity of magma below exsolution depths, relationship between magma-gas mixture density and water mass fraction, plots of eruption velocity as a function of initial water content of magmas.	Wilson and Head (1981, pp. 2974, 2983, Eqs. 16–18)	Sections 6.3.1, 6.3.3, Figs. 3, 4
Review of studies on the volume fraction of gas in a magma at which the magma fragments.	Discussion of magma fragmentation criteria.	Mader (1998, pp. 55–56)	Section 6.3.2
Data on volumes and durations of scoria (cinder) cone-forming eruptions.	Constraints on duration of potential volcanic eruptions in Yucca Mountain Region.	Wood (1980, p. 402)	Section 6.3.4
Duration and power output of explosive eruptive phases at Cerro Negro, Hekla, Tolbachik, Paricutin, and Heimaey volcanoes.	Calculation of mass discharge rates of explosive eruptive phases.	Jarzemba (1997, p. 136)	Section 6.3.4
Bulk grain size for eruptions at Cerro Negro, Tolbachik, and Mount Etna.	Estimation of statistics of grain size distributions for explosive basaltic eruptions.	Maleyev and Vande-Kirkov (1983, pp. 61–62); Rose et al. (1973, p. 342); McGetchin et al. (1974, p. 3264)	Section 6.5.1
Estimated bulk density of pyroclastic fallout deposits.	Recommendations for treatment of bulk deposit density in consequence analyses.	Blong (1984, p. 208); Sparks et al. (1997, p. 366)	Section 6.5.3

## **4.2 CRITERIA**

No criteria applicable to this analysis have been identified. This AMR complies with the DOE interim guidance (Dyer 1999). Subparts of the interim guidance that apply to this analysis are those pertaining to the characterization of the Yucca Mountain site (Subpart B, Section 15), the compilation of information regarding geology of the site in support of the License Application (Subpart B, Section 21(c)(1)(ii)), and the definition of geologic parameters and conceptual models used in performance assessment (Subpart E, Section 114(a)).

## **4.3 CODES AND STANDARDS**

No codes or standards apply to this analysis, which involves no design or construction.

INTENTIONALLY LEFT BLANK

## 5. ASSUMPTIONS

Our analyses are based on the assumption that a plausible future eruption (during the postclosure performance period) would be of the same character as Quaternary basaltic eruptions in the Yucca Mountain region (YMR). Eruptive styles and magmatic composition recorded at the Lathrop Wells volcano, the most recent in the region, are emphasized. Another overall assumption is that the event probabilities established in CRWMS M&O (2000c) pertain to the formation of a new volcano, and that a new volcano will contain some combination of scoria cone, spatter cones, and lava cones on the surface, and one or more dikes in the subsurface. Assumptions specific to each component of this report are described in the main text of Section 6 and are summarized below with corresponding section numbers.

1. *Assumption:* Data from analog sites provide a basis for estimating probability distributions related to the dimensions and geometry of volcanic plumbing for a plausible future (during postclosure performance period) formation of a new volcano. For conduit diameter, information from Tolbachik and Grants Ridge volcanoes is used to constrain the mean and maximum values. Dike-width distribution is based on data from dikes exposed in the YMR. Probability distribution for the number of dikes that would accompany formation of a new volcano is drawn from data on YMR volcanoes and intrusive suites. This assumption is discussed in Section 6.1.

*Sources of assumed values:* Doubik and Hill (1999, pp. 60–61); Keating and Valentine (1998, p. 41); Woldegabriel et al. (1999, p. 392); Crowe et al. (1983, pp. 266, 272).

*Rationale:* Direct data on the plumbing of the Lathrop Wells volcano are not available, so either theoretical estimates or data from analog sites must be relied upon. Theoretical estimates are not as reliable as analog data because general theories that account for all the complexities of magma intrusion at shallow depth do not exist.

*Need for verification:* Verification is not required because this assumption is based on the best available information, as discussed in Section 6.1. Additional information would negligibly affect the analysis.

2. *Assumption:* The most likely future eruptive event will have a magmatic chemical composition that is adequately represented by the mean composition of products of the Lathrop Wells volcano. This assumption is discussed in Section 6.2.1.

*Rationale:* Lathrop Wells volcano is well characterized chemically and represents relatively violent eruptions in the YMR, therefore this assumption is conservative from a perspective of potential atmospheric dispersal of waste by an eruption.

*Need for verification:* Verification is not required because additional data should negligibly alter the mean composition values and, therefore, would not affect the conservatism inherent in the assumption.

3. *Assumption:* Information on inferred eruptive styles, mineralogy, and crystallinity of Quaternary YMR basalts, combined with experimental studies on magmas of similar composition, constrain the water content of a plausible future eruption. This assumption is discussed in Section 6.2.2.

*Sources of assumed values:* Knutson and Green (1975, Fig. 1, p. 126); Sisson and Grove (1993a, pp. 163, 167).

*Rationale:* Direct measurements of pre-eruptive water content of magmas is very difficult, particularly at extinct volcanoes such as the YMR basaltic centers. The best approach would be to measure water contents in glass inclusions in phenocrysts, although even this method does not necessarily provide complete information on pre-eruptive water content. Furthermore, to the knowledge of the authors, such data do not exist for YMR basalts. Therefore, the less direct estimates using this assumption must be relied on.

*Need for verification:* Verification is not needed because this assumption uses the best available information, as described in Section 6.2.2. Additional information should negligibly affect the analysis.

4. *Assumption:* Gas compositions from active volcanoes (Mt. Etna, Momotomgo, Poas, Kilauea, Adoukoba, Erta Ale, Nyiragongo, and Surtsey) provide a basis for estimating gas composition of a potential new volcano in the YMR. This assumption is discussed in Section 6.2.3.

*Sources of assumed values:* Symonds et al. (1994, Tables 3–5).

*Rationale:* Absence of gas composition data for YMR basalts precludes the use of site-specific information. The volcanoes listed above define a range of basaltic composition that brackets the YMR basalt values. Therefore, the range of gas composition for these volcanoes should include the composition of a potential new eruption in the YMR.

*Need for verification:* Verification is not needed because this assumption is based on the best available information, as described in Section 6.2.3.

5. *Assumption:* Pressure in dikes and conduits during eruption is equal to lithostatic pressure. This assumption is discussed in Section 6.3.2.

*Sources of assumed values:* Jaupart and Tait (1990, p. 219).

*Rationale:* Actual pressure is a complex function of the velocity and density of the magma as it rises, and of the strength of wall rocks. Because a general model for these effects does not exist, lithostatic pressure is used as a first-order approximation.

*Need for verification:* Verification is not needed because this assumption is based on the best available approach, as discussed in Section 6.3.2.

6. *Assumption:* The flow of rising magma can be considered homogeneous and characterized by equilibrium between melt and exsolved volatiles. This assumption is discussed in Section 6.3.2.

*Rationale:* Actual velocities of melt and bubbles (exsolved volatiles) are different, but a general theory for basaltic magmas is not yet available to account for this effect.

*Need for verification:* Verification is not needed because this assumption is based on the best available approach, as discussed in Section 6.3.2.

7. *Assumption:* Fragmentation of rising magma occurs when the volume fraction of bubbles exceeds 0.75. This assumption is discussed in Section 6.3.2.

*Sources of assumed values:* Mader (1998, pp. 55–56).

*Rationale:* This is an established value in the peer-reviewed literature but is used only as an approximate value.

*Need for verification:* Verification is not needed because this assumption is based on the best available approach, as discussed in Section 6.3.2.

8. *Assumption:* Data on duration, power output, and grain size of historic eruptions of non-YMR volcanoes provide a basis for estimating power and duration of a future YMR eruption. This assumption is discussed in Sections 6.3.4. and 6.5.1.

*Sources of assumed values:* Crowe et al. (1983, pp. 266, 272); Wood (1980, p. 402); Jarzempa (1997, p. 136); Maleyev and Vande-Kirkov (1983, pp. 61–62); Rose et al. (1973, p. 342); McGetchin et al. (1974, p. 3264).

*Rationale:* As no direct data are available for these parameters for explosive eruption phases at YMR volcanoes, analog information must be used.

*Need for verification:* Verification is not needed because this assumption is based on the best available approach, as described in Sections 6.3.4 and 6.5.1.

9. *Assumption:* Methods, equations, and discussions in the peer-reviewed literature relating to calculations of magma viscosity, density, velocity, and discharge rates and of deposit density represent the best inputs to estimate these parameters for a new volcano.

*Sources of assumed values:* Shaw (1972, pp. 873, 878); Ochs and Lange (1999, p. 1314, Eq. 2); Rowland and Walker (1990, p. 626); Wilson and Head (1981, pp. 2974, 2983, Eqs. 16–18); Blong (1984, p. 208); Sparks et al. (1997, p. 366).

*Rationale:* As no direct data are available for eruptions at YMR volcanoes, approaches from the peer-reviewed literature must be used.

*Need for verification:* Verification is not needed because this assumption is based on the best available approach, as described in Sections 6.2.4, 6.3, 6.3.1, 6.3.3, and 6.5.3.

## 6. ANALYSIS/MODEL

### 6.1 CHARACTERISTICS OF ERUPTIVE CONDUITS, DIKE WIDTHS, AND DIKE SWARMS

Most observed basaltic eruptions begin as fissure eruptions, discharging magma where a dike intersects the Earth's surface, and they rapidly become focused into semicircular conduit eruptions. Some eruptions, such as Paricutin in Mexico (Luhr and Simkin 1993, p. 62), originated from single-point sources, although the vent was located on a long fissure that opened just before eruption began. The fissure is likely the surface expression of an ascending dike that fed the eruptions. Because of the effect of the (1) conduit diameter and (2) depth (to which a conduit extends before merging into a simple feeder dike) on the number of waste packages disrupted by a potential eruption at Yucca Mountain, it is important to constrain both these variables.

The best potential data for these parameters would come from a study of basaltic volcanic necks exposed by erosion in the southwestern United States where direct measurements of conduit diameter and its variation with depth could be made. However, such data are lacking; although many volcanic necks have been mapped as part of regional studies, they were not measured in detail, at least for the range of compositions of interest to the YMP. Without access to direct measurements of conduit diameter, estimates of this parameter are based on analog studies (see Section 5, Assumption 1).

Doubik and Hill (1999, pp. 60–61) proposed that the Lathrop Wells conduit may have been as wide as 50 m at depths equivalent to repository depth during the last stages of eruption. Their estimate was derived from an inferred analogy with modern eruptions at Tolbachik (Kamchatka, Russia). The conceptual model is that conduit diameter increases during successive stages of an eruption and that the maximum diameter achieved near the end of an eruption is the value of this parameter to be considered in evaluating volcanic disruption of a nuclear waste repository. The method for calculating conduit diameter of the Tolbachik volcanic vents is based on estimates of eruption volume, xenolith content of the pyroclastic deposits, and source depths of the xenoliths. By assuming an initial conduit diameter and calculating the volume of country rock removed along part of the length of the conduit, one can calculate the progressive enlargement of the conduit as the eruption proceeds.

The 50-m estimate of conduit diameter for Lathrop Wells is large, considering that Doubik and Hill (1999, p. 59) calculated a 48-m diameter for the Tolbachik conduit developed during a much larger eruption. This result is forced by their assumption that xenoliths at Lathrop Wells were derived only from a 550-m thick Tertiary ignimbrite section (compared to a 1.7-km source section at Tolbachik; Doubik and Hill 1999, pp. 57, 59), so that the erupted volume of xenoliths was derived from a shallower (but wider) conduit.

In the absence of specific data to test the assumptions made by Doubik and Hill (1999, p. 59), 50 m is suggested as a median value for conduit diameter at depth for potential eruptions at Yucca Mountain. The maximum value for the conduit diameter in the distribution to be used for performance assessment (PA) is 150 m, which corresponds to the diameter of the Grants Ridge

conduit/plug in New Mexico (Keating and Valentine 1998, p. 41; WoldeGabriel et al. 1999, p. 392). The large size of the Grants Ridge plug reflects that it erupted a volume on the order of a few km<sup>3</sup> of alkali basalt and, therefore, is expected to be a conservative upper bound for conduit diameter (compared, for example, to the Lathrop Wells volcano with its approximate volume of 10<sup>8</sup> m<sup>3</sup>; Crowe et al., 1983, p. 269) for a potential Yucca Mountain eruption. The minimum conduit diameter value for a PA realization should be the same as the dike width selected for that realization. The distribution should be log normal. This distribution will conservatively capture the range of conduit diameters for a potential volcanic event at Yucca Mountain.

Dike widths should be described with a log normal distribution with a minimum of 0.5 m, a mean of 1.5 m, and a 95th percentile width of 4.5 m. This distribution is consistent with data reported by Crowe et al. (1983, p. 266), who measured dikes in the YMR.

Volcanoes in the YMR are fed by one main dike along which a central cone and other vents may form, but subsidiary dikes are also present. For example, the Lathrop Wells volcano likely is underlain by three dikes (inferred from Perry et al. 1998, Figure 2.10): (1) the dike that fed the main cone and small spatter vents in a chain to the north and south of the cone, (2) a dike that fed spatter and scoria mounds in a parallel chain just to the east of the main dike, and (3) possibly a dike that fed scoria vents near the northern edge of the volcano. In addition, there are likely to be small dikes that radiate outward from the main cone's feeder conduit. The Paiute Ridge intrusive complex, which appears to have fed at least one volcanic vent (evidenced by the presence of lava-flow remnants and a plug-like body), may have as many as 10 dikes, in addition to sill-like bodies (as inferred from examination of Perry et al. 1998, Figures 5.15 and 5.16). To account for the likelihood of dike swarms, rather than single dikes, during formation of a new volcano, a log normal distribution is recommended for the number of dikes that has a minimum value of 1, a mean of 3 (reflecting our assumption that the most likely new volcano will be similar to the Lathrop Wells volcano), and a 95th percentile value of 10 (treating Paiute Ridge as a large event).

## 6.2 CHARACTERISTICS OF IGNEOUS MATERIAL

### 6.2.1 Magma Chemistry

Magma-chemistry data are used to determine parameters for important variables such as magmatic viscosity, magma temperature, and density. Two approaches are possible for predicting the chemistry of future magmas. The first is to calculate a volume-weighted mean composition based on analysis of basaltic rocks from the YMR, which is a method that would capture the existing magma chemistry record. A second approach is to use the most recent eruption at Lathrop Wells volcano as the one that most likely represents the composition of future eruptions. The second approach was selected because it emphasizes the composition that produced more violent explosive eruptions compared to other YMR volcanoes (as inferred from Perry et al. 1998, Chapter 2); therefore, it is the more conservative of the two approaches because it represents a greater potential dispersal of radionuclides (see Section 5, Assumption 2).

The major element variation for Lathrop Wells is based upon 45 chemical analyses (DTN LA00000000099.002). Table 2 gives the statistical parameters associated with these analyses.

Table 2. Mean Lathrop Wells Lava Chemistry with Associated Statistics  
(All values except count are in weight percent)

<b>SiO<sub>2</sub></b>		<b>TiO<sub>2</sub></b>		<b>Al<sub>2</sub>O<sub>3</sub></b>	
Mean	48.50	Mean	1.93	Mean	16.74
Standard Error	0.09	Standard Error	0.01	Standard Error	0.03
Median	48.57	Median	1.93	Median	16.75
Mode	48.55	Mode	1.97	Mode	16.87
Standard Deviation	0.58	Standard Deviation	0.06	Standard Deviation	0.22
Sample Variance	0.34	Sample Variance	0.00	Sample Variance	0.05
Count	45.00	Count	45.00	Count	45.00
<b>Fe<sub>2</sub>O<sub>3</sub>T<sup>a</sup></b>		<b>Fe<sub>2</sub>O<sub>3</sub><sup>b</sup></b>		<b>FeO<sup>b</sup></b>	
Mean	11.63	Mean	1.74	Mean	8.90
Standard Error	0.03	Standard Error	0.00	Standard Error	0.02
Median	11.58	Median	1.74	Median	8.86
Mode	11.56	Mode	1.73	Mode	8.84
Standard Deviation	0.22	Standard Deviation	0.03	Standard Deviation	0.17
Sample Variance	0.05	Sample Variance	0.00	Sample Variance	0.03
Count	45.00	Count	45.00	Count	45.00

DTN: LA000000000099.002

NOTES: <sup>a</sup> Total iron is reported as Fe<sub>2</sub>O<sub>3</sub>T  
<sup>b</sup> Fe<sub>2</sub>O<sub>3</sub> and FeO were recalculated assuming a 0.15 mole fraction of ferric iron (Fe<sub>2</sub>O<sub>3</sub>)

Table 2 (continued). Mean Lathrop Wells Lava Chemistry with Associated Statistics

MnO		MgO		CaO	
Mean	0.17	Mean	5.83	Mean	8.60
Standard Error	0.00	Standard Error	0.02	Standard Error	0.03
Median	0.17	Median	5.83	Median	8.55
Mode	0.17	Mode	5.88	Mode	8.41
Standard Deviation	0.00	Standard Deviation	0.11	Standard Deviation	0.22
Sample Variance	0.00	Sample Variance	0.01	Sample Variance	0.05
Count	45.00	Count	45.00	Count	45.00
Na <sub>2</sub> O		K <sub>2</sub> O		P <sub>2</sub> O <sub>5</sub>	
Mean	3.53	Mean	1.84	Mean	1.22
Standard Error	0.01	Standard Error	0.01	Standard Error	0.00
Median	3.55	Median	1.84	Median	1.22
Mode	3.59	Mode	1.84	Mode	1.21
Standard Deviation	0.09	Standard Deviation	0.04	Standard Deviation	0.03
Sample Variance	0.01	Sample Variance	0.00	Sample Variance	0.00
Count	45.00	Count	45.00	Count	45.00

DTN: LA000000000099.002

NOTE: The following sample analyses from Perry and Straub (1996, Appendix A) were used to develop the statistics in this table: LW11FVP, LW12FVP, LW74FVP, LW45FVP, LW72FVP, LW73FVP, LW100FVP, LW120FVP, LW121FVP, LW30FVP, LW31FVP, LW32FVP, LW63FVP, LW64FVP, LW65FVP, LW66FVP, LW67FVP, LW110FVP, LW115FVP, LW20FVP, LW21FVP, LW22FVP, LW23FVP, LW06FVP, LW07FVP, LW40FVP, LW41FVP, LW44FVP, LW55FVP, LW56FVP, LW19FVP, LW25FVP, LW26FVP, LW27FVP, LW28FVP, LW29FVP, LW04FVPA, LW54FVP, LW57FVP, LW58FVP, LW05FVPA, LW59FVP, LW60FVP, LW61FVP, LW62FVP.

## 6.2.2 Water Content

Eruptive styles in the YMR ranged from violent strombolian on one end of the spectrum to quiescent aa lava on the other as indicated by geologic mapping (Perry et al. 1998, Chapter 2). Eruption style is primarily controlled by volatile content (which is dominated by water) and the rate at which volatiles are exsolved from the magma. The observed eruptive styles indicate a large range in volatile contents and, hence, water of YMR magmas. In addition, variations in energy are suggested at individual volcanic centers such as those of the Quaternary Crater Flat field and Lathrop Wells volcanoes.

Amphibole, possibly of magmatic origin, is found as a rare and sparse phase in some Quaternary Crater Flat basalts. Knutson and Green (1975, Figure 1, p. 126), performing experiments on material similar in composition to YMR basalts, observed that magmatic amphibole was stabilized at water contents between 2 and 5 weight percent (wt%). Baker and Eggler (1983, p. 387) showed that at 2 Kbar pressure, water content in excess of 4.5 wt% is required to stabilize amphibole in high-alumina basalt similar to YMR basalts. However, water content substantially greater than 5 wt% is not considered likely because this high water content is most commonly

associated with more chemically evolved magmatic compositions than observed at the YMR. Also, Sisson and Grove (1993a, p. 167) note that low-Mg basalts with high alumina content cannot erupt as liquids with water content in excess of 4 wt% (by mass) because they will exsolve liquid and rapidly crystallize to form phenocryst-rich magmas as they approach the surface. Based on this, it is argued that 4 wt% is an upper bound on initial dissolved water content. Aa lava, on the other hand, may form from relatively low-volatile-content eruptions.

Even if one could tie a particular concentration of volatiles to a particular eruptive style, the YMR post-Miocene record is sparse; therefore, it is difficult to define rigorously a probability distribution function for water content for use in PA (see Section 5, Assumption 3). The following distribution is recommended:

From 0 to 1 wt% water, probability increases linearly such that magma with 0 wt% water has a zero probability of occurrence. This reflects our knowledge that very low volatile contents are very rare. Between 1 and 3%, the probability should be uniform, reflecting that this is the most likely range of water contents but that more specific information is not available. Between 3 and 4 wt%, the probability should decrease linearly so that it is zero at 4 wt%, representing the expectation that at about 4 wt%, basaltic magmas will crystallize underground rather than erupt.

Direct measurements of water in mafic magmas or magmatic products from a range of tectonic settings indirectly support the recommended parameter values and cover the range of values that can be reasonably expected for future basaltic igneous activity. Garcia et al. (1989, Table 1, p. 10527), Byers et al. (1985, Figure 4, p. 1891), and Muenow et al. (1979, Table 1, p. 74) found total water contents in Hawaiian tholeiites and transitional alkalic basalts that range from near 0 to nearly 1%. These melts probably represent higher degrees of partial melting than YMR basalts, so their low water contents are expected. On the other hand, Gaetani et al. (1993, pp. 332–334) and Sisson and Grove (1993b, p. 163) present experimental evidence that high-alumina basalt and basaltic andesite magmas commonly contain up to several percent by mass of water. Sisson and Layne (1993, Table 1, p. 622) measured water contents in glass inclusions from arc basalts and basaltic andesites that range from 1 to 6%. True magmatic values could be somewhat lower because of concentration of water in the inclusions, which is caused by partial crystallization of the melt after entrapment. Water contents of 0.2 to 2% have been reported for back arc basin lavas and 1.2 to 3% for island arc tholeiites and boninites (Danyushevsky et al. 1993, Tables 1 and 4, pp. 349 and 358).

### **6.2.3 Mole Percent of Constituents in Volcanic Gas**

A survey of data compilations from the literature, including volcanoes from convergent, divergent, and hot-spot tectonic settings, must suffice to constrain the gas constituents in YMR basalts owing to the absence of current activity in the YMR from which gases could be directly sampled. Two types of data exist in the literature: (1) measurements of emitted volcanic gases and (2) measurements of gases trapped in volcanic glass, or melt inclusions. The first type of data is more directly relevant to eruptive scenarios at Yucca Mountain because the gases released from an igneous event will include corrosive species. Also, gases will fractionate between the

magma and the gas phase during exsolution. Consequently, gas composition data for glasses may not directly represent their relative abundances in the gas phase after exsolution.

Measured concentrations of volcanic-gas constituents were taken from a compilation by Symonds et al. (1994, Tables 3–5), and only the data for mafic centers were included in the present analysis (see Section 5, Assumption 4). Data include hawaiite from Mt Etna; tholeiitic basalt from Momotombo, Poas, Kilauea, Ardoukoba, and Erta Ale; nephelinite from Nyiragongo; and alkali basalt from Surtsey (Table 3). The Table 3 statistics were calculated by first computing the mean for each of the above mentioned volcanic centers from the data in Symonds et al. (1994, Tables 3–5) and then using these individual means to generate the overall statistics.

Table 3. Mole Percent Concentration of Volcanic Gases and Associated Uncertainty Estimates

	H <sub>2</sub> O	H <sub>2</sub>	CO <sub>2</sub>	CO	SO <sub>2</sub>
MEAN	73.16	1.17	14.28	0.57	9.45
SQRRT SUM SQR <sup>a</sup>	17.97	0.89	16.03	0.59	8.90
STD DEV <sup>b</sup>	19.81	0.67	15.32	0.75	8.95
	S <sub>2</sub>	HCl	HF	H <sub>2</sub> S	fO <sub>2</sub> <sup>c</sup>
MEAN	0.41	0.87	0.17	0.74	-10.63
SQRRT SUM SQR <sup>a</sup>	0.63	0.21	0.04	1.04	1.92
STD DEV <sup>b</sup>	0.40	1.12	0.08	0.69	1.80

Source: Symonds et al. (1994, Tables 3 through 5)

NOTES: <sup>a</sup> square root of the sum of the squares of individual standard deviations for individual volcanic centers.

<sup>b</sup> standard deviation of the individual means for individual volcanic centers

<sup>c</sup> fO<sub>2</sub> is listed as log bars.

This is a closed data set, indicating that each parameter (other than fO<sub>2</sub>) must vary between 0 and 100%. Clearly, a species such as H<sub>2</sub>O will rarely be present at levels less than 50% and probably has some mean or median value of geologic significance. If data from sufficient eruptions and individual volcanoes were gathered, a normal distribution of values seems likely. As for the minor species, which are also corrosive, the cited uncertainties are quite large relative to mean values. Thus, it seems likely that adequate conservatism will be accommodated by a normal, or even a uniform, distribution.

#### 6.2.4 Magmatic Temperatures, Viscosities, and Densities

Magmatic temperature is a function of pressure, major-element composition, and water content. Many direct measurements of magmatic temperatures have been made for erupting lavas. However, this is only possible where water contents are low enough, or rates of magmatic outgassing are slow enough, to permit direct measurement. Thus, although direct measurements are available for the low end of the spectrum of water content, experiments must be relied on to

constrain magmatic temperatures for magmas with elevated water content (see Section 5, Assumption 9).

YMR basaltic lavas are generally aphyric to sparsely porphyritic (Perry and Straub 1996, p. 6), which indicates that they erupted at near-liquidus or superliquidus temperatures. The liquidus for dry basaltic magmas has a positive slope and varies as a function of pressure. Wet liquids, however, have negative slopes, so that water-bearing magmas may exist at a temperature less than that of the dry liquidus. Jaupart and Tait (1990, p. 219) present a simple expression for the solubility of water in basaltic magma

$$n = 6.8 \times 10^{-8} P^{0.7} \quad (\text{Eq. 1})$$

where  $n$  is the mass fraction of water and  $P$  is the pressure in Pascals. Because of the negative slope of the basalt solidus, corresponding temperatures on the solidus represent minimum liquidus temperatures. As magmas decompress, not only will they tend to exsolve more fluid, they will also tend to crystallize. A magma is saturated with respect to water when the pressure is such that  $n$  equals the initial water content. Table 4 shows saturation pressures, calculated from Equation 1, for initial water contents of 0.5, 1.0, 2.0, 3.0, and 4.0 wt% (wt% = 100 times the mass fraction). At lower pressures, water vapor would begin to exsolve and form bubbles (see also Section 6.3.2 below).

Using saturation pressures derived from Table 4, the following expression of Sisson and Grove (1993a, p. 178) can be used to estimate multiple phase-saturation (liquidus) temperatures in the magmas:

$$T(^{\circ}\text{C}) = 969 - (33.1 \times H_2O) + 0.0052 (P_b - 1) + 742.7 \times Al^{\#} - 138 \times NaK^{\#} + 125.3 \times Mg^{\#} \quad (\text{Eq. 2})$$

where  $H_2O$  is the wt% of water,  $P_b$  is pressure in bars (note that elsewhere in this document pressure is in Pascals),  $Al^{\#}$  is the ratio of mass fractions of  $Al_2O_3/(Al_2O_3 + SiO_2)$ ,  $NaK^{\#}$  is the ratio of mass fractions of  $(Na_2O + K_2O)/(Na_2O + K_2O + CaO)$ , and  $Mg^{\#}$  is molar  $Mg/(Mg + 2Fe_2O_3T)$ . It should be noted that  $Al^{\#}$ ,  $NaK^{\#}$ , and  $Mg^{\#}$  do not vary as a function of water content in Lathrop Wells magmas as these parameters simply express relative proportions.

Liquidus temperatures for Lathrop Wells magmas with different hypothetical water contents were calculated as follows. First, the mean Lathrop Wells composition (from Table 2) was normalized to 100% (anhydrous). Then, major element oxides were renormalized to sum to 99.5, 99.0, 98.0, 97.0, and 96.0 wt%. To these values were added 0.5, 1.0, 2.0, 3.0, and 4.0 wt%  $H_2O$ , respectively, so that the sum of the renormalized major element oxide content and the water content sum to 100 wt% in each case. With these new hypothetical compositions, and the saturation pressure calculated as described above, Equation 2 was used to compute the liquidus temperatures shown in Table 4. The same hypothetical compositions and calculated temperatures were used to calculate bubble- and crystal-free viscosity using the method of Shaw (1972, pp. 873, 878).

Density can also be calculated as a function of composition (including water content), pressure, and temperature using the formulation and data of Lange and Carmichael (1990, Table 3) with additional data for H<sub>2</sub>O (Ochs and Lange 1999, pp. 1314–1315). Equation 2 from Ochs and Lange (1999, p. 1315) produces the molar volume of the silicate liquid, which only requires a simple conversion to density. The density conversion can be done as follows: Assume that 100 g of magma are present. In doing the calculation, one converts the weight of each oxide (which is just the wt%) to the number of moles of each constituent. These terms can be summed to give a total number of moles. The density is then equal to the inverse of the product of molar volume (cm<sup>3</sup>/mol) and number of moles per 100 g of liquid. This result, in g/cm<sup>3</sup>, can then be converted to kg/m<sup>3</sup> as shown in Table 4.

Table 4. Calculated Saturation Pressures and Temperatures as a Function of Water Content for Lathrop Wells Magmas

Water Content (wt%)	Saturation Pressure (Pa)	Liquidus Temperature (°C)	Viscosity (log poise)	Density (kg/m <sup>3</sup> )
0	1 × 10 <sup>5</sup>	1169	2.678	2663
0.5	9.0 × 10 <sup>6</sup>	1153	2.572	2633
1	2.4 × 10 <sup>7</sup>	1137	2.472	2605
2	6.5 × 10 <sup>7</sup>	1106	2.284	2556
3	1.2 × 10 <sup>8</sup>	1076	2.112	2512
4	1.7 × 10 <sup>8</sup>	1046	1.957	2474

Derived using mean Lathrop Wells compositions from Table 2.

A review of some relevant experimental data reveals these values are reasonable. The temperature between 1174 and 1188°C is the liquidus temperature for a mildly alkalic basalt similar in composition to the mean Lathrop Wells lava composition (Sample 1 of Mahood and Baker (1986); composition of Sample 1 is reported in Table 7, and liquidus temperature is the temperature above which there are no mineral phases in Table 1 of that paper) and close to the temperature reported by Knutson and Green (1975, Figure 1) for a hawaiite that is also similar in composition to Lathrop Wells. Yoder and Tilley (1962, Figure 28) published results for water-saturated liquidus for a high-alumina basalt. At 1.75 × 10<sup>8</sup> Pa water pressure, the liquidus was more than 100°C cooler than the 10<sup>5</sup> Pa liquidus temperature. Thus, our calculated parameter values are consistent with a well- and long-established body of experimental data.

### 6.3 ERUPTIVE PROCESSES

Quaternary basalts of the YMR display textural and depositional facies that indicate a range of eruptive processes. Explosive processes, in which fragments, clots, or melt were erupted in a stream of gas, are evidenced by the presence of scoria cones and remnants of ash fallout blankets. Effusive processes, in which magma fragmentation did not occur in the feeding system, are recorded by the presence of lava flows, although it is also common in basaltic eruptions to produce lava flows by the coalescence and remobilization of explosively erupted clasts. Within these two broad categories of eruptive facies (explosive and effusive), there are further distinctions. Explosively erupted deposits, for example, may display a range of facies

depending on the local rate of accumulation and on the temperature of clasts when they are deposited. Very high accumulation rates of hot (still molten) clasts result in coalescence and formation of lava flows. Somewhat lower accumulation rates and temperatures may result in welded spatter, in which relicts of individual clast shapes may still be observed to varying degrees. Still lower accumulation rates and temperatures (such that the clasts are still plastic upon deposition) result in partly welded spatter, in which clast shapes are quite obvious but the deposit is resistant to erosion. Low accumulation rates of very hot clasts result in individual spatter clasts that flatten upon deposition but solidify before subsequent clasts are deposited on top and; therefore, do not weld. Deposits of nonindurated, brittle cinders (or scoria) result from deposition of already-cooled clasts. All of these explosive facies are present to some degree in the Yucca Mountain basalts. Effusive lava flows in the YMR are mainly of the aa type, indicating relatively high effusion rates (greater than c.  $1.5\text{--}3 \times 10^4$  kg/s; Rowland and Walker 1990, p. 626) (see Section 5, Assumption 9), although the limited extent of the flows suggests relatively short eruption duration.

The Lathrop Wells volcano is a good example of a range of eruptive processes recorded by a single volcano (Perry et al. 1998, Chp. 2). The surface of the main cone is composed mainly of loose scoria with a relatively high vesicularity. The cone is surrounded, particularly to the south, west, and north, by a fallout blanket up to c. 3 m thick (within 1 km of the cone) composed of the same loose scoria. Remnants of this fallout deposit are exposed northward up to 2 km from the crater, and ~20 km north of the crater, where its reworked equivalent is exposed in trenches excavated across the Solitario Canyon fault (Perry et al. 1998, pp. 4.24–4.30). These features all suggest a relatively high-energy eruption with an ash column that rose kilometers into the air so that clasts were cool when they fell to the ground and finer ash was dispersed widely by winds (termed a “violent strombolian eruption” by many volcanologists). Other parts of the Lathrop Wells volcano were emplaced by quite different mechanisms. For example, mounds of coarse, partially welded spatter indicate a local, relatively low-energy strombolian eruption. Recent quarry exposures reveal welded scoria and agglutinate, typical of a strombolian eruption, in the main cone, raising the possibility that only the late stages of the cone-forming eruptions were violent strombolian. Thick, stubby aa flows suggest short-duration, high-mass-flux effusive eruption. Other volcanoes of the YMR (e.g., Sleeping Butte, Red Cone, Black Cone) are less well preserved, but they seem to exhibit a similar range in eruptive styles at individual centers. This observation means that it is not representative to assume one eruption mechanism and, therefore, one exposure pathway for volcanic disruption of a potential repository.

The solubilities of volatiles such as H<sub>2</sub>O and CO<sub>2</sub> in basaltic magmas are proportional to pressure. At depth (for example, in a magma chamber), magmas will have relatively high volatile contents, but as they ascend through progressively lower lithostatic pressure, they will become oversaturated and bubbles will nucleate. Continued rise results in increasing numbers and sizes of bubbles (caused by combined exsolution of volatiles and decompression and coalescence growth of the bubbles); these two processes increase the specific volume of the magma, and as a consequence, its velocity also increases gradually (according to conservation of mass). Explosive eruption occurs when, at shallow depths, the magma reaches a foamy state and, with further decompression, it fragments, switching from being a melt with dispersed bubbles to a gas with dispersed fragments or clots of melt. At and above this fragmentation depth, the gas-melt mixture accelerates rapidly until it leaves the volcanic vent at speeds of tens

to a few hundreds of meters per second. A further complication in this sequence of events is the possibility of loss of volatiles through the walls of the conduit or dike as magma ascends. This action can reduce the effective volatile content for the eruption.

The dynamics of magma ascent and particularly the fragmentation process are currently a topic of intense research in the volcanological community. Most recent advances in this area focus on silicic rather than basaltic magmas. The reasons for this are twofold. First, silicic magmas are responsible for the most explosive eruptions and present the most severe hazard to populations; understanding their dynamics is key in mitigating these hazards. Second, silicic magmas have viscosities several orders of magnitude higher than basaltic magmas. This condition reduces greatly the effects of bubbles rising more rapidly than their host melts and coalescing with each other. Thus, theoretical modeling is made more tractable by having to consider only nucleation, decompression growth, and growth by diffusion of exsolving volatiles into bubbles. In other words, the dynamics are closely approximated by a "homogeneous flow" approach, in which the gas and melt move at about the same velocity everywhere and are in thermal equilibrium. Unfortunately, the rise of basaltic magmas with their lower viscosities is complicated by the potential for rapid rise and coalescence of bubbles (Vergnolle and Jaupart 1986, pp. 12842–12846). Extreme results of this process are represented by classic strombolian bursts, which are basically large bubbles rising through and bursting at the top of a magma column, producing eruptions of mostly gas with small amounts of melt (fragments of bubble walls) thrown out ballistically. Another example is the Hawaiian fire fountain eruptions, which have been observed to erupt mixtures with H<sub>2</sub>O vapor content much higher than the H<sub>2</sub>O solubility at depth. A general theory for the rise of basaltic magmas, accounting fully for the important two-phase flow effects, does not exist. Instead, the treatment relied on below simplifies the problem by assuming homogeneous flow.

### 6.3.1 Magma Ascent Rate Below Volatile Exsolution

Wilson and Head (1981) developed a theory for the ascent of basaltic magmas along dikes and cylindrical conduits using the homogeneous flow simplification. At depth, where magma is under sufficient pressure that all volatiles are dissolved, the buoyancy-driven ascent velocity,  $u_f$ , is

$$u_f = \frac{A\eta}{4K\rho_m r} \left[ \left( 1 + \frac{64gr^3(\rho_c - \rho_m)K\rho_m}{A^2\eta^2} \right)^{1/2} - 1 \right] \quad (\text{Eq. 3})$$

where  $A = 64$  (circular conduit) or  $24$  (dike),  $\eta$  is magma viscosity,  $K = 0.01$ ,  $\rho_m$  is the melt density (no bubbles),  $\rho_c$  is the wall rock density,  $r$  is the conduit radius or dike half width, and  $g$  is gravitational acceleration (Wilson and Head 1981, p. 2974) (see Section 5, Assumption 9). Note that flow described in Equation 3 can occur only when  $\rho_c > \rho_m$ .

### 6.3.2 Volatile Exsolution and Fragmentation

As magmas rise, volatiles may begin to exsolve. The solubility of water ( $n$ ), the major volatile species in basalt, is approximated by Equation 1 (Jaupart and Tait 1990, p. 219). The depth at

which exsolution of water vapor begins to occur is the depth at which the magma becomes saturated with respect to its original water content, which, assuming lithostatic pressure ( $P = \rho_c g d$ , where  $d$  is depth; see Section 5, Assumption 5), can be derived as:

$$d_{\text{exs}} = \frac{(n_i / 6.8 \times 10^{-8})^{10/7}}{\rho_c g} \quad (\text{Eq. 4})$$

where  $d_{\text{exs}}$  is exsolution depth in meters (m),  $n_i$  is the initial dissolved mass fraction of water at the magma's depth of origin,  $\rho_c$  is the average density of the crust above  $d_{\text{exs}}$  in  $\text{kg/m}^3$ , and  $g$  is gravitational acceleration ( $\text{m/s}^2$ ). This relation is plotted in Figure 1. The mass fraction of water exsolved from a basaltic magma,  $n_{\text{exs}}$ , at a given depth is

$$n_{\text{exs}} = n_i - n \quad \text{when } d < d_{\text{exs}} \quad (\text{Eq. 5a})$$

$$n_{\text{exs}} = 0 \quad \text{when } d > d_{\text{exs}} \quad (\text{Eq. 5b})$$

The density of the mixture of silicate melt and water vapor bubbles ( $\rho_{\text{mix}}$ ) can be calculated from (Wilson and Head 1981, p. 2973)

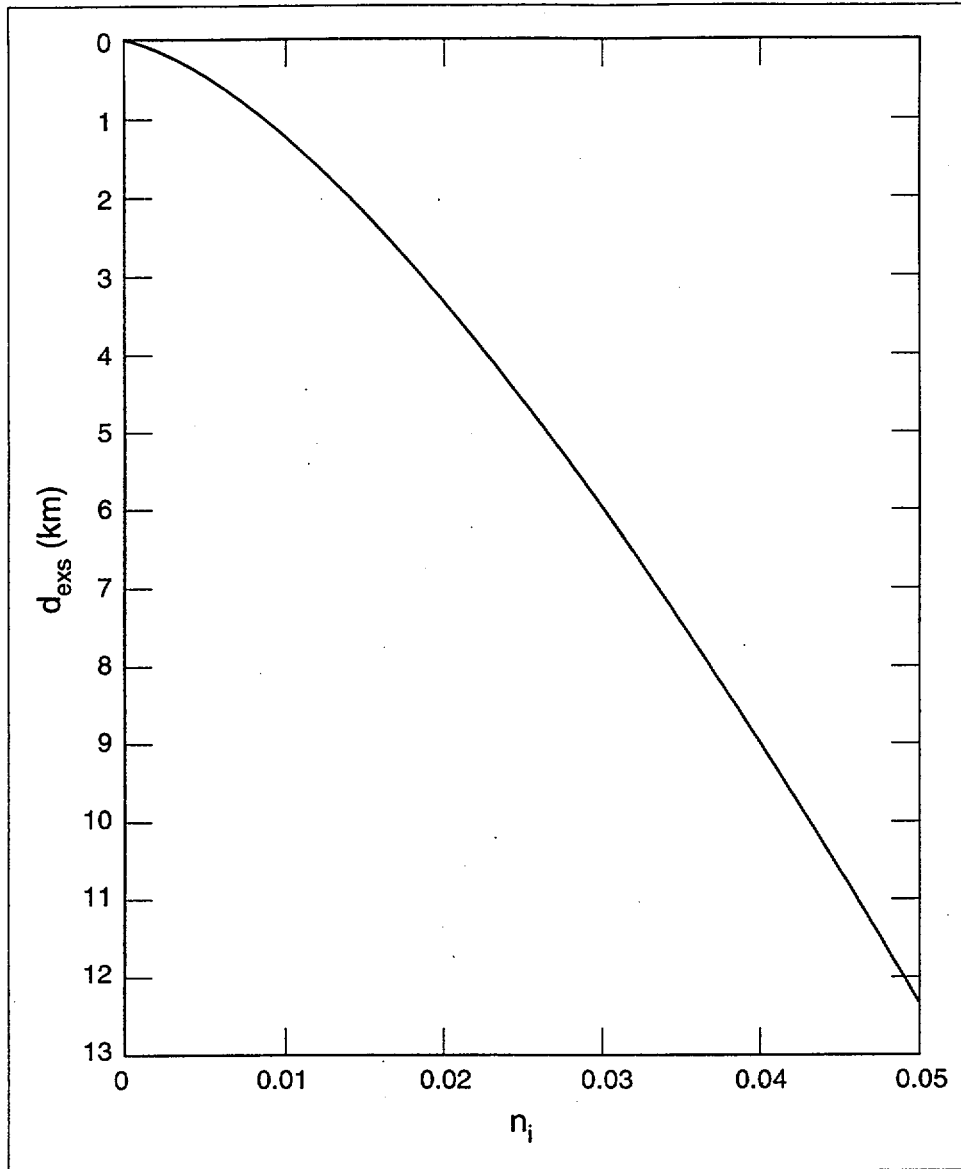
$$\frac{1}{\rho_{\text{mix}}} = \frac{n_{\text{exs}}}{\rho_g} + \frac{(1 - n_{\text{exs}})}{\rho_m} \quad (\text{Eq. 6})$$

The density of the gas phase ( $\rho_g$ ) can be calculated using the ideal gas law,

$$\rho_g = \frac{P}{RT} \quad (\text{Eq. 7})$$

where  $R$  is the gas constant for water (in this report, a value of 461 J/kg-K is used) and  $T$  is temperature. If it is assumed that the pressure in a conduit or dike is determined by the lithostatic pressure,  $\rho_g$  can be computed as a function of depth  $d$ :

$$\rho_g = \frac{\rho_c g d}{RT} \quad (\text{Eq. 8})$$



DTN: N/A (plot of Equation 4)

NOTE: The calculations assume that pressure in the magma column is lithostatic and that bubble nucleation kinetics can be ignored. The average (shallow) crustal density ( $\rho_c$ ) is taken to be  $2000 \text{ kg/m}^3$ , as an example.

Figure 1. Plot of the Depth at Which Volatile ( $\text{H}_2\text{O}$ ) Exsolution Begins ( $d_{\text{exs}}$ ) for Initial Dissolved Water Content ( $n_i$ ) up to 0.05

Equations 1 and 4 to 8 can be used to calculate the mixture density for any initial volatile content at any depth, which may be useful for estimating the interactions between the mixture and the repository. The mixture density can also be expressed in terms of gas volume fraction,  $\phi$ , as

$$\rho_{mix} = \phi\rho_g + (1 - \phi)\rho_m \quad (\text{Eq. 9})$$

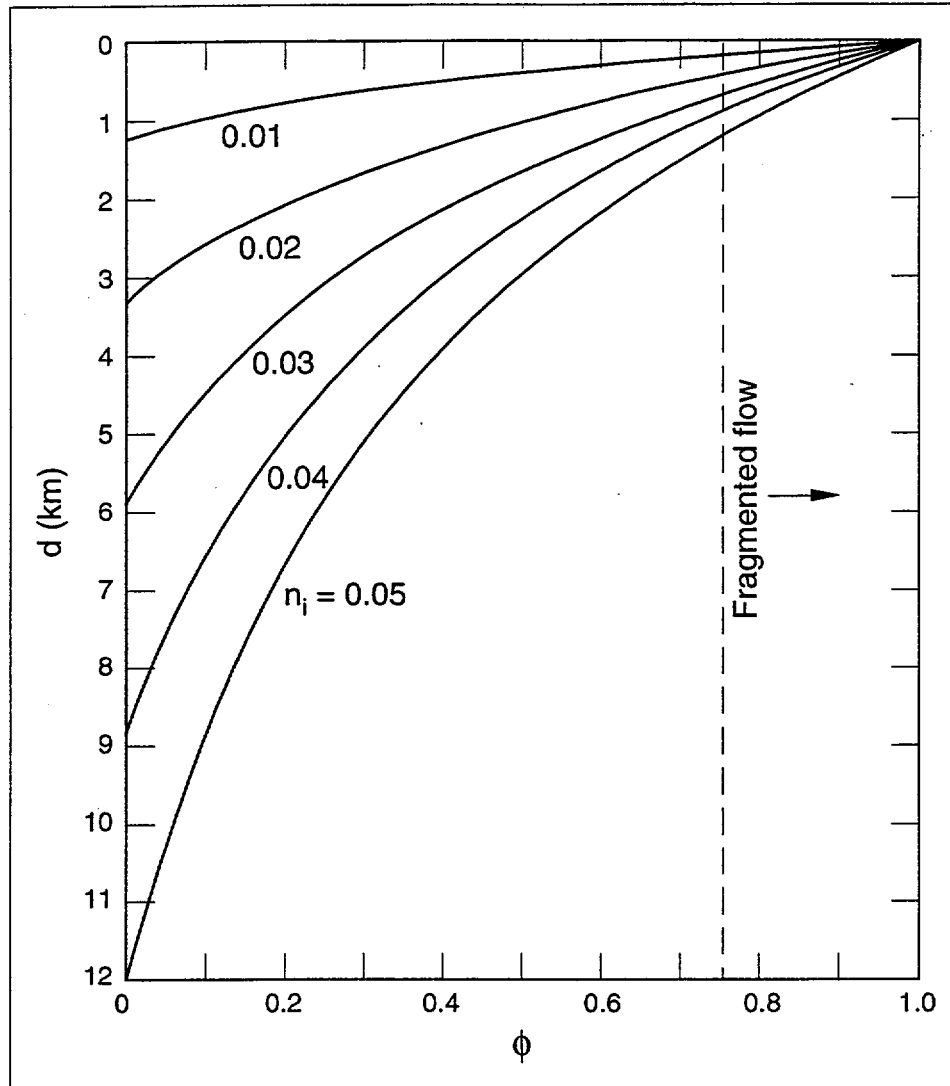
Rearranging, the gas volume fraction is here derived as:

$$\phi = \frac{\rho_{mix} - \rho_m}{\rho_g - \rho_m} \quad (\text{Eq. 10})$$

Figure 2 shows the depth at which fragmentation occurs in rising basalt, assuming that:

1. The flow is steady and homogeneous, the system is closed (no gas loss into country rock), and bubble nucleation and growth kinetics can be ignored (see Section 5, Assumption 6).
2. The vertical pressure profile in the dike/conduit below the fragmentation depth is very close to the lithostatic pressure profile (see Section 5, Assumption 5).
3. A gas volume fraction at which fragmentation commences can be established.

The limitations of the first assumption have already been discussed. The second assumption is very good at depths where  $\phi$  is small, but it becomes less accurate toward the fragmentation depth, and it is probably very inaccurate above the fragmentation depth. However, the second assumption is a good estimate of the “average” fragmentation depth for a variety of different scenarios. The third assumption is currently a subject of intense research. A critical value of  $\phi$  at which fragmentation occurs has commonly been assumed to be close to 0.75 (Mader 1998, p. 55), and this is adopted in Figure 2. Recent studies have demonstrated, however, that fragmentation can take place in a range from  $0.60 < \phi < 0.95$  (for example, Mader 1998, p. 56). The commonly assumed critical fragmentation value of  $\phi_{crit} = 0.75$  is adopted as a reasonable estimate given how little is understood about this process, particularly with regard to basaltic magmas (see Section 5, Assumption 7). With all these assumptions, Figure 2 illustrates that estimated fragmentation depths for initial volatile contents between 0 and 4 wt% ranges from about 0 to 900 m.



DTN: N/A (plot of Equation 10)

NOTE: Calculations assume  $\rho_c = 2000 \text{ kg/m}^3$ ,  $\rho_m = 3000 \text{ kg/m}^3$ ,  $T = 1300 \text{ K}$ , and  $R = 461 \text{ J kg/K}$ . The dashed line defines a critical gas volume fraction of 0.75, which in this report is assumed to be the threshold for fragmentation of the magma. Plot is derived by solving Equations 1 and 5 as functions of depth for a given value of  $n_i$ , Equations 8 and 6, and finally Equation 10 for each value of  $n_i$ .

Figure 2. Plot of the Variation of Gas Volume Fraction ( $\phi$ ) with Depth ( $d$ ), Assuming Pressure in the Magma is Lithostatic, for Initial Dissolved Water Content  $n_i = 0.01, 0.02, 0.03, 0.04,$  and  $0.05$ .

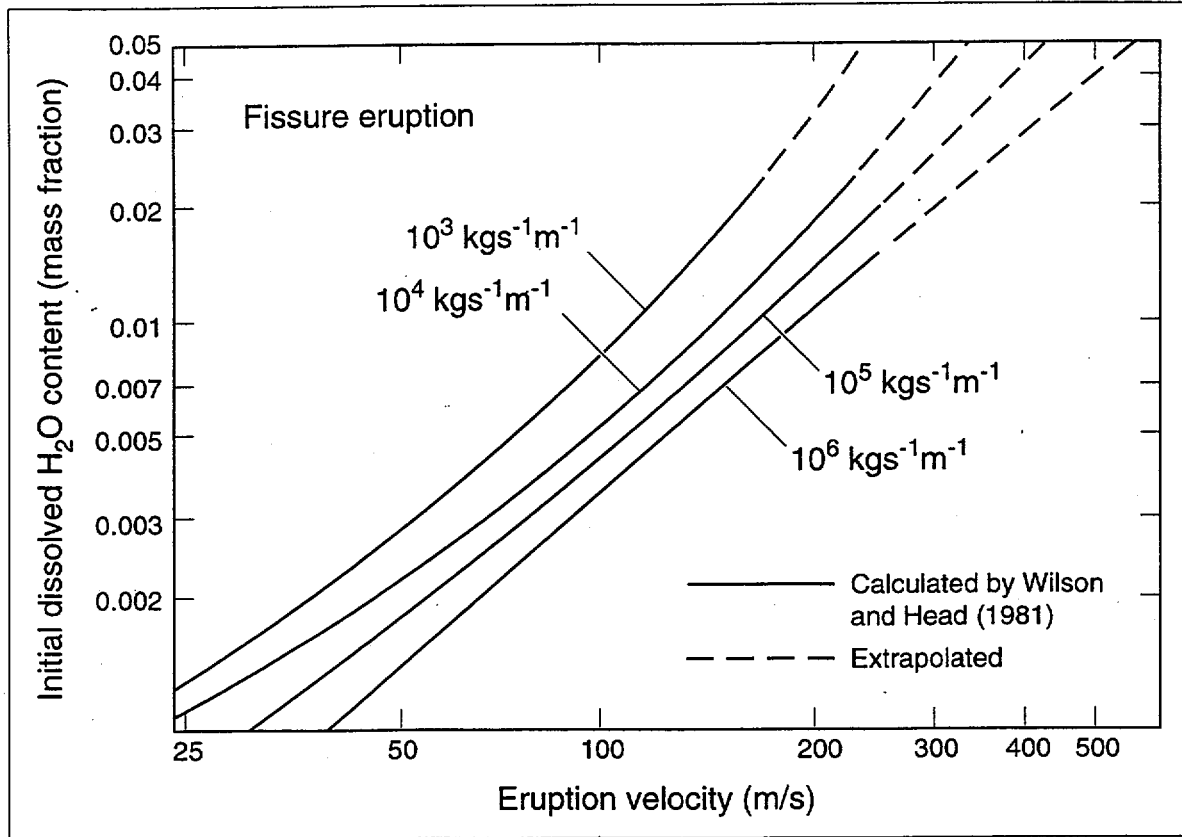
### 6.3.3 Velocity as a Function of Depth Above $d_{exs}$

Descriptions of the magma velocity, conduit/dike dimensions, and magma pressure as functions of  $d$  require, even with the homogeneous flow approximation and a steady-state assumption, solution of three coupled equations (Wilson and Head 1981, Equations 16, 17, and 18 on p. 2974). Two of these equations are ordinary differential equations. Detailed solution of these equations for a range of parameters appropriate to volcanism in the YMR is beyond the scope of this report. However, Wilson and Head (1981, p. 2983) do provide some plots that relate eruption velocity,  $u_{erupt}$ , (where the magma-gas mixture exits the vent) to initial dissolved water content ( $n_i$ ) of the magma, assuming that the pressure in the conduit/dike is equal to lithostatic pressure. Their solutions, shown with the solid curves in Figures 3 and 4, are for values of  $n_i$  up to approximately 0.02 for both dike (fissure) and circular conduit geometries. As discussed in Section 6.2.2, it is possible that  $n_i$  values for basalts of the YMR have been as high as 0.03 to 0.04, and the possibility of values as high as 0.05 is allowed in these plots. It is expected that YMR basaltic magmas with such high water contents would not erupt (Section 6.2.2). Thus, Figures 3 and 4 show the extrapolated values (dashed parts of the curves) for velocity at these higher initial water contents. Note that these are only graphical extrapolations, not actual solutions to the governing equations. However, given the various simplifications that are made in arriving at the Wilson and Head (1981, p. 2983) results, these extrapolations are reasonable approximations (see Section 5, Assumption 9).

The velocity of magma ascending from some depth to the vent probably can be estimated with sufficient accuracy for PA by simplifying such that velocity increases linearly from  $0.01u_{erupt}$  at  $d_{exs}$  to  $0.1u_{erupt}$  at the fragmentation depth, thence increasing linearly to  $u_{erupt}$  at the vent ( $u_{erupt}$  obtained from Figures 3 and 4). Using such an approach will account for the greater accelerations that are thought to occur above the fragmentation depth and the more gradual acceleration below it. In addition, this approach guarantees consistency in the calculations of velocity at various depths (as opposed to random sampling from distributions at different depths).

### 6.3.4 Eruption Duration and Volume

Eruption duration is difficult to estimate because, during the formation of a volcanic center, it is likely that eruptive discharge rates could have varied substantially. Wood (1980, p. 402) provides data on the duration of scoria-cone forming eruptions, showing that they range from one day to about 15 years, with a median value of 30 days. Wood (1980, p. 402) also states that about 93% of such eruptions last less than one year. Note that this duration is for formation of the entire volcano, including lava flows, scoria cone, and fallout blanket. As mentioned above, the aa character of the Lathrop Wells lava flows implies a mass discharge rate of at least  $3 \times 10^4$  kg/s. Using this value as a conservative minimum eruption rate, the Lathrop Wells volcano, with a total volume of about  $10^8 \text{ m}^3$  (Crowe et al. 1983, p. 269; mass of about  $3 \times 10^{11}$  kg calculated using an approximated magma density of  $2600 \text{ kg/m}^3$  from Table 4), would have erupted in about  $10^7$  s (about 120 days) if the eruption rate was maintained during that time. For comparison, the Hekla 1947 eruption reached discharge rates of about  $4.7 \times 10^7$  kg/s during highly explosive phases (Table 5). At this rate, which could be considered a reasonable



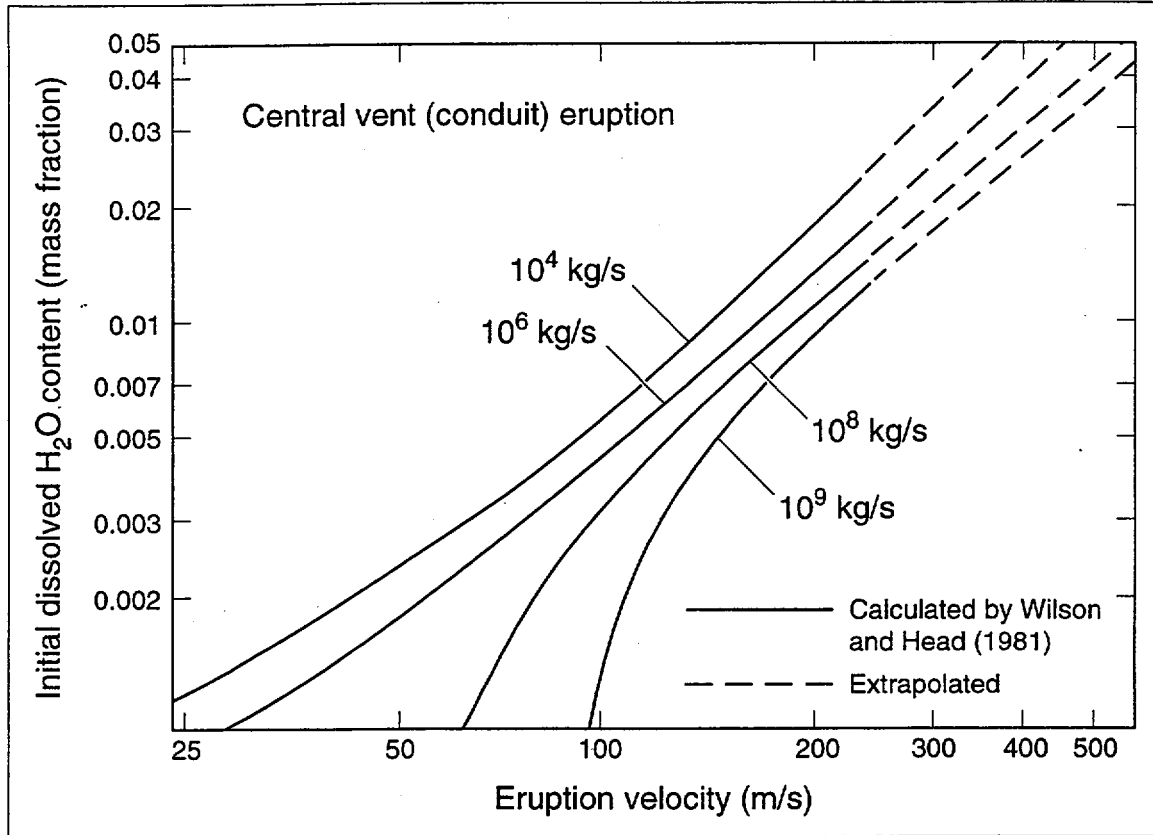
Source: Wilson and Head (1981); plot of equations from reference and extrapolations

NOTE: Solid curves show values calculated by Wilson and Head (1981, p. 2983), whereas dashed lines are graphical extrapolations to include the range of initial volatile contents of concern for Yucca Mountain. The Wilson and Head calculations assume homogeneous flow and lithostatic pressure in the rising magma column.

Figure 3. Plot of the Variation of Eruption Velocity ( $u_{erupt}$ ) with Initial Dissolved Water Content ( $n_i$ ) for Various Mass Discharge Rates Along a Fissure

maximum rate for volcanoes of the YMR, the Lathrop Wells volcano would have completely formed in about 1.8 hours, which is an unrealistically short time. For total eruption duration (formation of the entire volcano), a log normal distribution with a minimum of one day, a mean of 30 days, and a maximum of 15 years is recommended.

Total erupted volume can be obtained by multiplying eruption duration by mass discharge rate, and then dividing by magma density of  $2600 \text{ kg/m}^3$  (a representative density for magmas for a Lathrop Wells type eruption, see Table 4). This will result in a “dense rock equivalent” volume (often referred to as the DRE volume). The bulk volume of deposits from an eruption will be larger because of the presence of voids (vesicles) within particles and of void space between particles. For a violent strombolian eruption, the fallout blanket will have a density within a range specified below. If the bulk volume of a violent strombolian eruption is needed, then one should use the bulk density (see Section 6.5.3) instead of the magma density.



Source: Wilson and Head (1981); plot of equations 17 to 18 from reference and extrapolations

NOTE: Solid curves show values calculated by Wilson and Head (1981, p. 2983), whereas dashed lines are graphical extrapolations to include the range of initial volatile contents of concern for Yucca Mountain. The Wilson and Head calculations are based on the assumption of homogeneous flow and lithostatic pressure in the rising magma column.

Figure 4. Plot of the Variation of Eruption Velocity ( $U_{erupt}$ ) with Initial Dissolved Water ( $n_i$ ) Content for Various Mass Discharge Rates from a Circular Conduit.

Table 5. Explosive Eruptive Events, Duration, and Power and Estimated Mass Discharge Rates Used to Develop Probability Distributions for Eruptive Plume Dispersal Calculations

Event	Log (t) (t in s) <sup>a</sup>	Log (Po) (Po in W) <sup>a</sup>	Mass Discharge Rate (kg/s) <sup>b</sup>
Cerro Negro, 1992	4.8	12.0	$7.4 \times 10^5$
Hekla, 1970	3.9	12.8	$4.7 \times 10^6$
Tolbachik, 1975	6.1	11.7	$3.7 \times 10^5$
Paricutin, 1944 I	5.6	11.1	$9.3 \times 10^4$
Paricutin, 1944 II	6.8	11.5	$2.3 \times 10^5$
Paricutin, 1946	6.8	9.0	$7.4 \times 10^2$
Hekla, 1947	3.3	13.8	$4.7 \times 10^7$
Heimaey, 1973	6.4	9.9	$5.9 \times 10^3$

Sources: <sup>a</sup>Jarzemba (1997, p. 136)

<sup>b</sup>Mass discharge rates based on  $T = 1350$  K and magma heat capacity  $c_p = 1000$  J/kg-K (Best 1982, p. 301). Mass discharge rate =  $Po(c_p T)^{-1}$ .

For the duration of individual explosive phases that produce a high column and disperse ash widely, we adopt the same range of parameter values used in Jarzempa (1997, pp. 136–137; see Section 5, Assumption 8). The data supporting this range are shown in Table 5, which also includes the estimated mass discharge rate for the eruptions, using an estimated magma specific heat of 1000 J/kg-K (see, for example, the range of values in Best 1982, p. 301) and temperature of 1350 K. Explosive phases lasted from about half an hour to 73 days. However, we note that the longer duration events occurred at volcanoes of larger volume than is typical of the YMR in the Quaternary. For example, Paricutin volcano is more than an order of magnitude larger in volume ( $2.1 \times 10^9 \text{ m}^3$ ; Wood 1980, p. 390) than the Lathrop Wells volcano.

#### 6.4 ENTRAINMENT OF RADIOACTIVE WASTE IN ASCENDING MAGMA

Quantification of the amount of waste that could be entrained by rising magma and subsequently erupted and dispersed is difficult because of uncertainties regarding the potential interactions of the magmatic system with the repository. Some of these uncertainties are volcanological in nature, and some are related to the nature of the engineered system; the latter are beyond the scope of this report.

Uncertainties are inherent in the following volcanic processes: (1) the interaction between a rising dike and the perturbed stress field around repository drifts; (2) the interaction between rising, vesiculating magma and the partially open drifts (for example, would magma run like lava flows for long distances down the drifts, would it pile up quickly to block the drift and therefore allow magma to continue rising, or would it explode down the drift?); and (3) the depth to which conduits might extend (that is, if a wide conduit is formed but extends only 200 m below the surface, then it will not have as large a disruptive effect on the potential repository).

There are a few data available on the interaction of magma with undisturbed country rock and subsequent eruption of the lithic debris for the range of eruptive styles that can be reasonably expected at Yucca Mountain. For example, Valentine and Groves (1996, pp. 79–84) report data on the quantity of wall rock debris erupted from various depths during strombolian, Hawaiian, effusive, and hydrovolcanic activity at two volcanoes. Hydrovolcanic eruptions reported by Valentine and Groves contained between 0.32 and 0.91 volume fraction of wall rock debris, with most of that originating in the uppermost ~510 m of the dike/conduit feeder systems. Strombolian, Hawaiian, and effusive eruptions ejected much lower volumes of wall rock debris, commonly resulting in total volume fractions of  $10^{-3}$  to  $10^{-5}$ . Studies of more sites, including those that probably produced violent strombolian eruptions, were not completed by YMP. Doubik and Hill (1999, p. 60) state that the Lathrop Wells volcano has a relatively high average lithic volume fraction of  $9 \times 10^{-3}$  for xenoliths > 1 mm, based on image analysis of unspecified locations. It is possible that all the locations studied by Doubik and Hill were located in a quarry that exposes proximal cone deposits. Clarification of this issue will require analysis of more exposures at Lathrop Wells and analysis of previously collected data. Addressing this issue may be important because Doubik and Hill (1999) cite similarity of lithic content as a justification for using the relatively large and violent Tolbachik eruptions as analogs for the Lathrop Wells volcano (and, hence, potential eruptions at Yucca Mountain).

## 6.5 ASH PLUMES AND THEIR DEPOSITS

### 6.5.1 Bulk Particle Size and Distribution of Deposits from Strombolian and Violent Strombolian Eruptions

As described in Section 6.3, explosive eruptive styles of Quaternary volcanoes in the YMR include both strombolian and violent strombolian. Strombolian eruptions are characterized by short-duration bursts that throw relatively coarse fragments of melt out on ballistic trajectories. Most of the fragments (clasts) are deposited immediately around the vent, with only a very small fraction of finer particles rising higher and being dispersed by wind to form minor fallout sheets. Table 6 shows estimated bulk eruptive grain-size distribution parameters for the Etna Northeast Crater eruptions of September 1971 (McGetchin et al. 1974, Figure 8, p. 3264). This result is probably representative of many strombolian eruptions, being skewed toward very coarse clast sizes.

Violent strombolian eruptions, on the other hand, are characterized by vertical eruption of a high-speed jet of a gas-clast mixture. As the eruptive mixture rises in the jet, it entrains and heats air, which in turn reduces the bulk mixture density until the jet becomes buoyant and continues to rise as a plume. The plume rises to an altitude of neutral buoyancy compared to the surrounding atmosphere, in which it then spreads laterally as an anvil or “umbrella” cloud that is transported downwind. Clasts fall out from both the vertical eruption column and from the umbrella cloud according to their settling velocities. Such an eruption tends to produce a fallout sheet with volume comparable to or as much as 13 times that of the cone (excluding lava flows; Crowe et al. 1983, p. 272). Historic violent strombolian eruptions at Paricutin produced a fallout sheet:cone volume ratio of about 4:1, and Sunset Crater (Arizona) produced a ratio of about 3.2:1 (Crowe et al. 1983, p. 272). Table 6 shows bulk eruptive grain-size distributions for three violent strombolian eruptions (Tolbachik and Cerro Negro, 1971 and 1968; Maleyev and Vande-Kirkov 1983, pp. 61–62; Rose et al. 1973, p. 342; see Section 5, Assumption 8). Mean clast diameters for these eruptions range from 0.19 to 0.37 mm, and standard deviations range from 1.5 to 2.5  $\Phi$  units ( $\Phi = -\log_2 d$ , where  $d$  is the particle diameter in mm). For comparison, Jarzempa (1997, p. 137) gives a log-triangular distribution with a minimum of 0.1 mm, a maximum of 100 mm, and a median of 1 mm.

Given the data in Table 6, and the fact that there are not many data available to constrain bulk particle size in violent strombolian eruptions, we suggest using a log triangular distribution for mean clast size, as Jarzempa (1997, p. 137) did, but have the minimum value be 0.01 mm, the mode at 0.1 mm, and the maximum value be 1.0 mm. This distribution more closely matches the data provided here.

Given a mean clast size, the standard deviation of the particle size is needed to provide ASHPLUME with sufficient information on the particle size distribution. Table 6 provides information on the graphic standard deviation  $\sigma_\phi$ , which is defined as

$$\sigma_\phi = (\Phi_{84} - \Phi_{16})/2 \quad (\text{Eq. 11})$$

where  $\Phi_{84}$  is the 84th percentile grain size and  $\Phi_{16}$  is the 16th percentile grain size expressed in  $\phi$  units. It is recommended that, for a given mean particle diameter,  $\sigma_\phi$  be sampled from a uniform distribution between  $\sigma_\phi = 1$  and  $\sigma_\phi = 3$ .

Table 6. Estimated Bulk Clast Size Distribution Parameters for Three Violent Strombolian Eruptions (Tolbachik and Cerro Negro 1971 and 1968) and One Strombolian Eruption (Etna 1971)

	Combined Great Tolbachik N. Breakthrough <sup>a</sup>	Cerro Negro 1971 (overall) <sup>b</sup>	Cerro Negro 1968 (overall) <sup>b</sup>	Bulk Etna Northeast Crater <sup>c</sup>
Median (mm)	0.3	0.24	0.15	95
Graphic Mean (mm)	0.37	0.23	0.19	110
Graphic Standard Deviation ( $\sigma_\phi$ )	2.5	1.5	1.83	3.48

Sources: <sup>a</sup> Derived from data presented in Maleyev and Vande-Kirkov (1983, pp. 61–62).

<sup>b</sup> Rose et al. (1973, p. 342).

<sup>c</sup> McGetchin et al. (1974, p. 3264).

### 6.5.2 Clast Characteristics

The clasts produced by strombolian and violent strombolian eruptions can be quite different in character. As can be seen in Table 6, strombolian eruptions produce a much higher proportion of coarse clasts, with the mean size commonly being  $> 10$  cm. Common strombolian clast types include ribbon, spindle, and cowpie bombs. Ribbon and spindle bombs take their shape as they are stretched and torn or as they spin through the air on their dominantly ballistic paths; these shapes indicate the hot, fluid state of the clasts during flight. Cowpie bombs are very hot and fluid when they hit the ground. All these clasts are hot during flight and deposition because of their large size (low surface-area-to-volume ratio minimizes heat loss) and low eruption height (they have less time to cool before hitting the ground). These large clasts may have vesicle (bubble) volume fractions up to  $\sim 70\%$ . Smaller clasts, in the mm to cm range, tend to be sub-equant vesicular scoria clasts, and they can have a range of vesicularities (for example, the Cinder Cone eruption at Lassen Volcanic National Park, California, produced scoria with vesicularities of 20 to 70%; Heiken and Wohletz 1985, p. 34). Finer ash-sized clasts tend to be less vesicular, and can range from irregular to fluidal to blocky in shape.

Violent strombolian eruptions carry clasts much higher in the air, providing more cooling time; the clasts cool more quickly because they have a much higher degree of fragmentation. A much larger proportion of the clasts is in the mm to cm size range compared to strombolian eruptions, and most of these clasts have irregular shapes and relatively high vesicularities.

In violent strombolian eruptions, the long-range, downwind transport and fallout of clasts becomes an important issue for YMP PA calculations. Transport and deposition of clasts depend on their settling velocity in air, which in turn depends on their bulk density (the melt density corrected for the porosity, or vesicularity, of the clasts) and shape. Calculations of clast dispersal

commonly use a shape factor,  $F = (b + c)/2a$ , where  $a$ ,  $b$ , and  $c$  are the lengths of the longest, medium, and shortest axes of the clasts. Clasts produced by these types of eruptions can have a range of shapes. Jarzempa (1997, p. 139) used a value of  $F = 0.5$  as a shape factor that is likely to be representative of common clast shapes, and in the absence of further data, we recommend this value for PA calculations for YMP.

Density of erupted particles varies with particle size because larger particles tend to have a higher fraction of vesicles (bubble voids) than small particles. Detailed data are lacking, but it is recommended that the particle density be varied as follows:

- For particle diameters less than or equal to 0.01 mm, the particle density is 0.8 of the magma density (which is taken to have an average value of  $2600 \text{ kg/m}^3$  for a Lathrop Wells-type magma). This is based on a fine-particles void fraction of 0.2 due to vesicles.
- For particle diameters greater than or equal to 10 mm, the particle density is 0.4 of the magma density. This is based on a void fraction of 0.6 due to vesicles.
- Between 0.01 mm and 10 mm, density should decrease linearly with increasing diameter.

### **6.5.3 Density of Fallout Deposits**

Bulk in-situ density of fallout deposits typically ranges from 300 to  $1500 \text{ kg/m}^3$  (Sparks et al. 1997, p. 366) but is rarely directly measured, particularly for basaltic deposits such as are most likely in the YMR. Blong (1984, p. 208) estimates that some fallout deposits have a density of approximately  $1000 \text{ kg/m}^3$ . There are two possible ways of treating deposit density in TSPA-SR calculations: (1) simply use  $1000 \text{ kg/m}^3$  or (2) sample from a normal distribution of deposit densities ranging from 300 to  $1500 \text{ kg/m}^3$ , with a mean of  $1000 \text{ kg/m}^3$  (see Section 5, Assumption 9).

INTENTIONALLY LEFT BLANK

## 7. CONCLUSIONS

This AMR provides technical bases for parameters that will be used by PA related to the effects of a volcanic eruption through the potential Yucca Mountain repository. Uncertainties in the parameters are described in the text as appropriate. The information in this AMR is based largely on literature values and simple calculations.

The following specific parameter distributions are suggested:

- Conduit diameter – Log normal distribution, minimum diameter equal to dike width, median diameter equal to 50 m, maximum value 150 m.
- Dike width – Log normal distribution, minimum of 0.5 m, mean of 1.5 m, 95th percentile value of 4.5 m.
- Number of dikes associated with formation of a new volcano – Log normal distribution with minimum of 1, mean of 3, 95th percentile value of 10.
- Magma chemistry – Mean Lathrop Wells composition, Table 2.
- Water content of magmas – Uniform distribution between 1 and 3 wt%, zero probability of 0 wt% increasing linearly to 1 wt%, zero probability of 4 wt% with linear distribution between 3 and 4 wt%.
- Gas composition – Derived from a suite of active volcanoes, Table 3.
- Magmatic temperatures, viscosities, and densities – Calculated from theoretical relations, Table 4. Liquidus temperature ranges from 1046 to 1169°C, viscosity ranges from 1.957 to 2.678 (log poise units), density ranges from 2474 to 2663 kg/m<sup>3</sup>.
- Magma ascent rate below vesiculation depth – Equation 3.
- Volatile exsolution depths – Figure 1, range from about 9 km to zero depth for water contents between 0 and 4 wt%.
- Fragmentation depths – Figure 2, range from 0 to 900 m (approximately) for water contents between 0 and 4 wt%.
- Velocity as a function of depth – Eruption velocity  $u_{erupt}$  is estimated from Figures 3 and 4. Velocity then decreases linearly downward to  $0.1u_{erupt}$  at the fragmentation depth. Below fragmentation depth the velocity continues to decrease linearly to  $0.01u_{erupt}$  at the depth where water exsolution begins.
- Eruption duration – For formation of an entire volcano, a log normal distribution with a minimum of one day, a mean of 30 days, and a maximum of 15 years. Duration and volume of individual explosive phases during formation of a new volcano should be a probability distribution function derived from Table 5, with a cutoff so that sampled

volumes or the sums of sampled volumes do not exceed the sampled volume of the whole volcano.

- Mean particle size erupted during violent strombolian phases – Log triangular distribution with a minimum of 0.01 mm, a mode of 0.1 mm, and a maximum of 1.0 mm.
- Standard deviation of particle size distribution for a given mean – Uniform distribution between  $\sigma_\phi = 1$  and  $\sigma_\phi = 3$ .
- Clast characteristics – Shape factor of 0.5.
- Density of erupted particles – For particle diameters less than or equal to 0.01 mm, density is 0.8 of the magma density. For particles greater than 10 mm, density is 0.4 of the magma density. For particles between 0.01 and 10 mm, density should decrease linearly with increasing diameter.
- There are two possible ways of treating deposit density in TSPA-SR calculations – (1) Simply use 1000 kg/m<sup>3</sup> or (2) sample from a normal distribution of deposit densities ranging from 300 to 1500 kg/m<sup>3</sup>, with a mean of 1000 kg/m<sup>3</sup>.

The current qualification status of input data on major element composition of the Lathrop Wells volcanic center is qualified.

## 8. INPUTS AND REFERENCES

### 8.1 DOCUMENTS CITED

- Baker, D.R., and Eggler, D.H. 1983. "Fractionation Paths of Atka (Aleutians) High Alumina Basalt: Constraints from Phase Relations." *Journal of Volcanology and Geothermal Research*, 18, 387–404. Amsterdam, The Netherlands: Elsevier Science. TIC: 246252.
- Best, M.G., 1982. *Igneous and Metamorphic Petrology*. New York, New York: W.H. Freeman and Company, 630 pp. On order: Library Tracking Number 1612.
- Blong, R.J. 1984. *Volcanic Hazards, A Sourcebook on the Effects of Eruptions*. Sydney, Australia: Academic Press, 424 pp. TIC: 247016.
- Byers, C.D., Garcia, M.O., and Muenow, D.W. 1985. "Volatiles in Pillow Rim Glasses from Loihi and Kilauea Volcanoes, Hawaii." *Geochimica et Cosmochimica Acta*, 49, 1887–1896. New York, New York: Pergamon Press. TIC: 246241.
- Crowe, B.M., Self, S., Vaniman, D., Amos, R., and Perry, F. 1983. "Aspects of Potential Magmatic Disruption of a High-Level Radioactive Waste Repository in Southern Nevada." *Journal of Geology*, 91, (3), 259–276. Chicago, Illinois: University of Chicago Press. TIC: 216959.
- CRWMS M&O (Civilian Radioactive Waste Management System Management and Operating Contractor). 1999a. *Characterize Eruptive Processes at Yucca Mountain, NV*. TDP-CRW-GS-000003. Las Vegas, Nevada: CRWMS M&O. ACC:MOL.19990811.0287
- CRWMS M&O. 1999b. *Analysis to Characterize the Eruptive Processes at Yucca Mountain, Nevada*. Activity Evaluation, July 26, 1999. Las Vegas, Nevada: CRWMS M&O. ACC: MOL.19990917.0049.
- CRWMS M&O. 2000a. Input Transmittal from Total System Performance Assessment Department to Disruptive Events Department for Draft AMR—T0055 Number of Waste Packages Hit by Igneous Intrusions. 00209.T. Las Vegas, Nevada: CRWMS M&O. ACC: MOL.20000425.1065.
- CRWMS M&O. 2000b. *Igneous Consequences Modeling for the TSPA-SR*. ANL-WIS-MD-000017. Las Vegas, Nevada: CRWMS M&O. Submit to RPC: URN-0014.
- CRWMS M&O 2000c. *Input Transmittal from Disruptive Events Department to Disruptive Events Department for Draft AMR—T0015 Characterize Framework for Igneous Activity at Yucca Mountain, Nevada*. ANL-MGR-GS-000001. 00210.T. Las Vegas, Nevada: CRWMS M&O. ACC: MOL.20000412.0207.
- Danyushevsky, L.V., Falloon, T.J., Sobolev, A.V., Crawford, A.J., Carroll, M., and Price, R.C. 1993. "The H<sub>2</sub>O Content of Basalt Glasses from Southwest Pacific Back-Arc Basins." *Earth*

and *Planetary Science Letters*, 117, 347–362. Amsterdam, The Netherlands: Elsevier Science B.V. TIC: 246102.

DOE (U.S. Department of Energy). 2000. *Quality Assurance Requirements and Description*. DOE/RW-0333P, Rev. 9. Washington, D.C.: DOE Office of Civilian Radioactive Waste Management. ACC: MOL.19991028.0012.

Doubik, P., and Hill, B.E. 1999. “Magmatic and Hydromagmatic Conduit Development During the 1975 Tolbachik Eruption, Kamchatka, with Implications for Hazards Assessment at Yucca Mountain, NV.” *Journal of Volcanology and Geothermal Research*, 91, 43–64. Amsterdam, The Netherlands: Elsevier Science B.V. TIC: 246029.

Dyer, J.R. 1999. “Revised Interim Guidance Pending Issuance of New U. S. Nuclear Regulatory Commission (NRC) Regulations (Revision 01, July 22, 1999), for Yucca Mountain, Nevada.” Letter from J. R. Dyer (DOE/YMSCO) to D. R. Wilkins (CRWMS M&O), September 3, 1999, OL&RC:SB-1714, with enclosure, “Interim Guidance Pending Issuance of New NRC Regulations for Yucca Mountain (Revision 01).” ACC: MOL.19990910.0079.

Gaetani, G.A., Grove, T.L., and Bryan, W.B. 1993. “The Influence of Water on the Petrogenesis of Subduction-Related Igneous Rocks.” *Nature*, 365, 332–335. London, England: Macmillan Journals. TIC: 246792.

Garcia, M.O., Muenow, D.W., Aggrey, K.E., and O’Neil, J.R. 1989. “Major-Element, Volatile, and Stable Isotope Geochemistry of Hawaiian Submarine Glasses.” *Journal of Geophysical Research*, 94, (B8), 10525–10538. Washington, D.C.: American Geophysical Union. TIC: 246240.

Heiken, G.H., and Wohletz, K. 1985. *Volcanic Ash*. Berkeley, California: University of California Press. TIC: 242991.

Jarzemba, M.S. 1997. “Stochastic Radionuclide Distributions after a Basaltic Eruption for Performance Assessments of Yucca Mountain.” *Nuclear Technology*, 118, 132–141. La Grange Park, Illinois: American Nuclear Society. TIC: 237944.

Jaupart, C., and Tait, S. 1990. “Dynamics of Eruptive Phenomena.” Chapter 8 of *Modern Methods of Igneous Petrology: Understanding Magmatic Processes*, Nicholls, J., and Russell, J.K., editors, pp. 211–238. Reviews in Mineralogy Volume 24. Washington, D.C.: Mineralogical Society of America. TIC: 246394.

Keating, G.N., and Valentine, G.A. 1998. “Proximal Stratigraphy and Syneruptive Faulting in Rhyolitic Grants Ridge Tuff, New Mexico, USA.” *Journal of Volcanology and Geothermal Research*, 81, 37–49. Amsterdam, The Netherlands: Elsevier Science B.V. TIC: 246096.

Knutson, J., and Green, T.H. 1975. “Experimental Duplication of a High-Pressure Megacryst/Cumulate Assemblage in a Near-Saturated Hawaiiite.” *Contributions to Mineralogy and Petrology*, 52, 121–132. Berlin, Germany: Springer-Verlag. TIC: 225057.

- Lange, R.L., and Carmichael, I.S.E. 1990. "Thermodynamic Properties of Silicate Liquids with Emphasis on Density, Thermal Expansion, and Compressibility." Chapter 2 of *Modern Methods of Igneous Petrology: Understanding Magmatic Processes*, Nicholls, J., and Russell, J.K., editors, pp. 25–59. Reviews in Mineralogy Volume 24. Washington, D.C.: Mineralogical Society of America. TIC: 246394.
- Luhr, J.F., and Simkin, T., eds. 1993. *Paricutin, The Volcano Born in a Mexican Cornfield*. Phoenix, Arizona: Geoscience Press. TIC: 247017.
- Mader, H.M. 1998. "Conduit Flow and Fragmentation." *The Physics of Explosive Volcanic Eruptions*, Gilbert, J.S., and Sparks, R.S.J., editors. Geological Society of London Special Publication No. 145, pp. 51–71. London, United Kingdom: Blackwell Scientific Publications. TIC: 247115.
- Mahood, G.A., and Baker, D.R. 1986. "Experimental Constraints on Depths of Fractionation of Mildly Alkalic Basalts and Associated Felsic Rocks: Pantelleria, Strait of Sicily." *Contributions to Mineralogy and Petrology*, 93, 251–264. New York, New York: Springer-Verlag. TIC: 225072.
- Maleyev, Ye.F., and Vande-Kirkov, Yu.V. 1983. "Features of Pyroclastics of the Northern Breakthrough of the Great Tolbachik Fissure Eruption and the Origin of its Pale-Grey Ash." *The Great Tolbachik Fissure Eruption*, Fedotov, S.A., and Markhinin, Ye.K., editors, pp. 57–71. Cambridge, England: Cambridge University Press. Copyright requested: Library Tracking Number 247236.
- McGetchin, T.R., Settle, M., and Chouet, B.A. 1974. "Cinder Cone Growth Modeled after Northeast Crater, Mount Etna, Sicily." *Journal of Geophysical Research*, 79, (23), 3257–3272. Washington, D.C.: American Geophysical Union. TIC: 246027.
- Muenow, D.W., Graham, D.G., Liu, N.W.K., and Delaney, J.R. 1979. "The Abundance of Volatiles in Hawaiian Tholeiitic Submarine Basalts." *Earth and Planetary Science Letters*, 42, 71–76. Amsterdam, The Netherlands: Elsevier Science. TIC: 246833.
- Ochs, F.A., III, and Lange, R.A. 1999. "The Density of Hydrous Magmatic Liquids." *Science*, 283, 1314–1317. Washington, D.C.: American Association for the Advancement of Science. TIC: 246839.
- Perry, F.V., and Straub, K.T. 1996. *Geochemistry of the Lathrop Wells Volcanic Center*. LA-13113-MS. Los Alamos, New Mexico: Los Alamos National Laboratory. ACC: MOL.19961015.0079.
- Perry, F.V., Crowe, B.M., Valentine, G.A., Bowker, L.M., editors. 1998. *Volcanism Studies: Final Report for the Yucca Mountain Project*. LA-13478. Los Alamos, New Mexico: Los Alamos National Laboratory. TIC: 247225.

- Rose, W.I., Jr., Bonis, S., Stoiber, R.E., Keller, M., and Bickford, T. 1973. "Studies of Volcanic Ash from Two Recent Central American Eruptions." *Bulletin Volcanologique*, XXXVII-3, 338–364. New York, New York: Springer-Verlag. TIC: 246073.
- Rowland, S.K., and Walker, G.P.L. 1990. "Pahoehoe and aa in Hawaii: Volumetric Flow Rate Controls the Lava Structure." *Bulletin of Volcanology*, 52, 615–628. New York, New York: Springer-Verlag. TIC: 246030.
- Shaw, H.R. 1972. "Viscosities of Magmatic Silicate Liquids: An Empirical Method of Prediction." *American Journal of Science*, 272, 870–889. New Haven, Connecticut: Yale University, Kline Geology Laboratory. TIC: 246470.
- Sisson, T.W., and Grove, T.L. 1993a. "Temperatures and H<sub>2</sub>O Contents of Low-MgO High-Alumina Basalts." *Contributions to Mineralogy and Petrology*, 113, 167–184. New York, New York: Springer-Verlag. TIC: 246251.
- Sisson, T.W., and Grove, T.L. 1993b. "Experimental Investigations of the Role of H<sub>2</sub>O in Calc-alkaline Differentiation and Subduction Zone Magmatism." *Contributions to Mineralogy and Petrology*, 113, 143–166. New York, New York: Springer-Verlag. TIC: 246909.
- Sisson, T.W., and Layne, G.D. 1993. "H<sub>2</sub>O in Basalt and Basaltic Andesite Glass Inclusions from Four Subduction-Related Volcanoes." *Earth and Planetary Science Letters*, 117, 619–635. Amsterdam, The Netherlands: Elsevier Science Publishers B.V. TIC: 246239.
- Sparks, R.S.J., Bursik, M.I., Carey, S.N., Gilbert, J.S., Glaze, L.S., Sigurdsson, H., and Woods, A.W. 1997. *Volcanic Plumes*. New York, New York: John Wiley & Sons, 574 pp. TIC: 247134.
- Symonds, R.B., Rose, W.I., Bluth, G.J.S., and Gerlach, T.M. 1994. "Volcanic-Gas Studies: Methods, Results, and Applications." Chapter 1 of *Volatiles in Magmas*. Reviews in Mineralogy Volume 30, Carroll, M.J., and Holloway, J.R., editors, pp. 1–66. Washington, D.C.: Mineralogical Society of America. TIC: 238061.
- Valentine, G.A., and Groves, K.R. 1996. "Entrainment of Country Rock During Basaltic Eruptions of the Lucero Volcanic Field, New Mexico." *Journal of Geology*, 104, 71–90. Chicago, Illinois: University of Chicago Press. TIC: 246146.
- Vergnolle, S., and Jaupart, C. 1986. "Separated Two-Phase Flow and Basaltic Eruptions." *Journal of Geophysical Research*, 91, (B12), 12842–12860. Washington, D.C.: American Geophysical Union. TIC: 239308.
- Wemheuer, R.F. 1999. "First Issue of FY00 NEPO QAP-2-0 Activity Evaluations." Interoffice correspondence from R.F. Wemheuer (CRWMS M&O) to R.A. Morgan (CRWMS M&O), October 1, 1999, LV.NEPO.RTPS.TAG.10/99-155, with attachments, Activity Evaluations. ACC: MOL.19991028.0162.

Wilson, L., and Head, J.W., III. 1981. "Ascent and Eruption of Basaltic Magma on the Earth and Moon." *Journal of Geophysical Research*, 86, (B4), 2971–3001. Washington, D.C.: American Geophysical Union. TIC: 225185.

WoldeGabriel, G., Keating, G.N., and Valentine, G.A. 1999. "Effects of Shallow Basaltic Intrusion into Pyroclastic Deposits, Grants Ridge, New Mexico, USA." *Journal of Volcanology and Geothermal Research*, 92, 389–411. Amsterdam, The Netherlands: Elsevier Science. TIC: 246037.

Wood, C.A. 1980. "Morphometric Evolution of Cinder Cones." *Journal of Volcanology and Geothermal Research*, 7, 387–413. Amsterdam, The Netherlands: Elsevier Scientific Publishing. TIC: 225565.

Yoder, H.S., Jr., and Tilley, C.E. 1962. "Origin of Basalt Magmas: An Experimental Study of Natural and Synthetic Rock Systems." *Journal of Petrology*, 3, (3), 342–532. London, England: Oxford University Press. TIC: 247024.

## **8.2 CODES, STANDARDS, REGULATIONS, AND PROCEDURES**

AP-3.10Q, Rev 2, ICN 0. *Analyses and Models*. Washington, D.C.: U.S. Department of Energy, Office of Civilian Radioactive Waste Management. ACC: MOL.200000217.0246.

DOE. 2000. *Quality Assurance Requirements and Description*. DOE/RW-0333P, Rev. 9. Washington, D.C.: DOE OCRWM. ACC: MOL.199910281.0012.

QAP-2-0, Rev. 5. *Conduct of Activities*. Las Vegas, Nevada: CRWMS M&O. ACC: MOL.19980826.0209.

QAP-2-3, Rev. 10. *Classification of Permanent Items*. Las Vegas, Nevada, CRWMS M&O. ACC: MOL.19990316.0006.

## **8.3 SOURCE DATA, LISTED BY DATA TRACKING NUMBERS**

LA000000000099.002. *Major Element, Trace Element, Isotopic, and Mineral Chemistry Data from Lathrop Wells*. Submittal date: 08/02/1995.

LAGV831812AQ97.001. *Magmatic Effect Data for Revision and Final Publication of the Volcanism Synthesis Report*. Submittal date: 08/29/1997.